Electronic Supplementary Information

for

Structure-activity relationships of aniline-based squaraines for distinguishable staining and bright two-photon fluorescence bioimaging in plant cells

Nan Zhang, Haixia Chang, Rong Miao, Taihong Liu,* Liping Ding and Yu Fang*

Key Laboratory of Applied Surface and Colloid Chemistry of Ministry of Education, School of Chemistry and Chemical Engineering, Shaanxi Normal University, Xi'an, Shaanxi 710119, P. R. China

Corresponding authors: liuth121@snnu.edu.cn (T. Liu); yfang@snnu.edu.cn (Y. Fang)

Contents

1. Experimental section

1.1. Materials and methods

All reagents and solvents were commercially available without further purification unless otherwise noted. Thin-layer chromatography (TLC) was performed on precoated silica gel 60 F254 plates. Column chromatography was performed over silica gel 230-400 mesh. NMR (^{1}H and ^{13}C) measurements were performed at room temperature by a Bruker Avance III NMR spectrometer with tetramethylsilane (TMS) as an internal reference. High-resolution mass spectra (HRMS) were acquired in atmospheric pressure chemical ionization (APCI) sources using a Bruker maXis UHR-TOF mass spectrometer. The optical properties of the fluorophores were investigated in the spectroscopic-grade solvents. Ultrapure water (resistivity >18.0 MΩ·cm) was obtained from a Millipore Milli-Q system. UV-vis spectra were recorded using a Shimadzu UV-2600 spectrometer in 10 mm path length quartz cuvettes. Steady-state fluorescence emission spectra were obtained using a fluorescence spectrometer (Edinburgh FLS980) with a xenon lamp as the light source at room temperature. Fluorescence lifetimes (τ_F) were determined by the time-correlated single photon counting technique (TCSPC) with the same Edinburgh spectrometer using a pulsed picosecond diode laser (EPL-635) as the excitation source. The instrument response function (IRF) was measured by monitoring a scattering solution of colloidal silica (Ludox). It should be mentioned that the maximum optical density of the investigated solutions did not exceed 0.1 and all reabsorption effects were negligible. The absolute fluorescence quantum yields (Φ_F) were obtained using a Hamamatsu C9920-02G instrument with a Xe excitation source and a Hamamatsu A10080-01 monochromator. Details of two-photon absorption (2PA) measurements could be found in the reported literatures by our group.[1,2]

1.2. Bioimaging studies

The fluorophores including squaraines (SQs), rhodamine B (RDB), fluorescein sodium (FLS), congo red, and Hoechst 33342 were evaluated properly. The images of plant cells (onion inner epidermis and

Arabidopsis seedlings) were achieved with a confocal laser scanning microscope (CLSM, Olympus FV1200) using 460 (FLS), 488 (RDB), 500 (congo red), and 635 nm (SQs) laser excitation. Cells and tissues incubated without the fluorophores acted as the controls. Briefly, the inner layer of a fresh thin onion was peeled off. Small pieces were cut and transferred to 20 mL distilled water in a petri dish. On a clean glass slide (24 × 50 mm), two drops of water were placed and 100 μL of SQs and Hoechst 33342 ($c \sim 1.0 \times 10^{-4}$ mol/L) were mixed well. Then the pieces of onion epidermal cells were placed on the microscopic slide at 37°C for 5 min, covered with a coverslip, and observed under the CLSM instrument. Biodistribution of the SQs in onion was imaged on the Bruker In-Vivo Xtreme Imaging System (In-Vivo Xtreme). Two-photon fluorescence microscopy (2PFM) images were obtained with a modified Leica SP8 DIVE microscope system. Cells tissues untreated with the fluorophores acted as the controls. Repeated experiments were carried out properly and standard errors were shown.

2. Synthesis and characterization

2.1. General procedures for synthesizing the SQs

The symmetrical SQs were generally prepared by reacting one equivalent of squaric acid with two equivalents of the electron-donating heterocycle in refluxing 1-butanol/toluene with an apparatus of Dean-Stark, where the generated water was removed continuously. The fluorophores SQ1 and SQ2 were synthesized according to the versatile and straightforward methods reported by the literatures.[3,4] The synthesis and purification details for SQ3 have been reported previously.[5,6]

2.2. Synthesis of the fluorophore SQ1

The synthesis details of the fluorophore SQ1 were presented in Scheme S1. The Boc-protection of piperidine-4-carboxylic acid was carried out based on the previously reported literatures.[7,8]

2.2.1. Synthesis of *tert*-butyl-4-(bis(2-ethylhexyl)carbamoyl)piperidine-1-carboxylate (1-A)

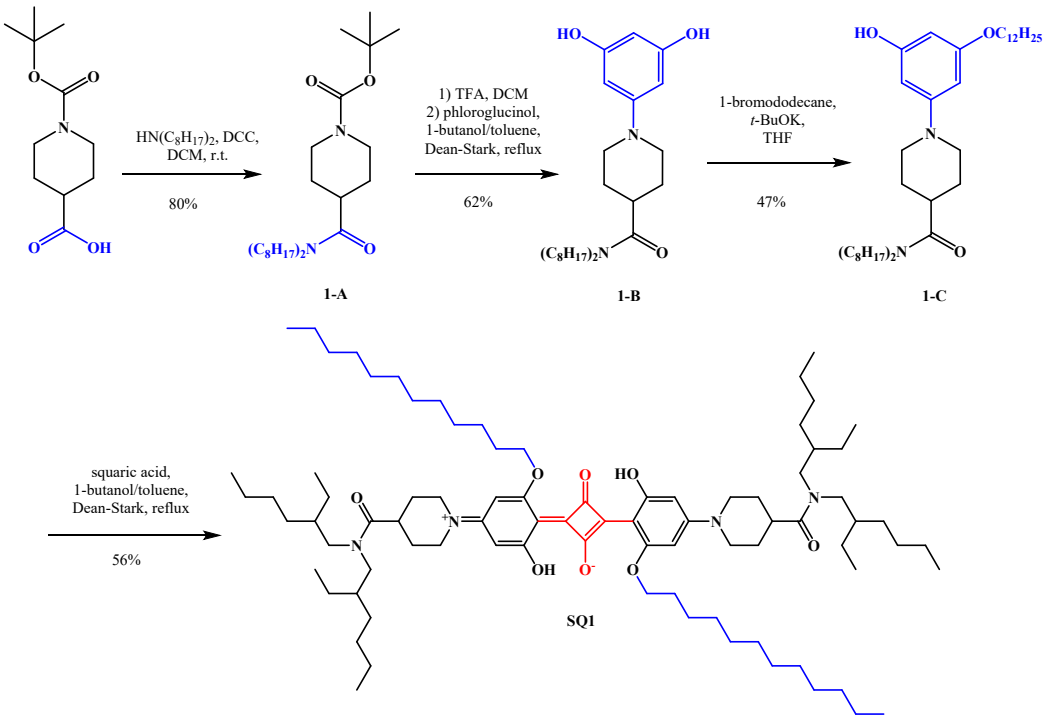

Scheme S1. Synthesis route for the fluorophore SQ1.

Boc-protected piperidine-4-carboxylic acid (5.0 g, 21.8 mmol), dicyclohexylcarbodiimide (DCC, 4.5 g, 21.8 mmol), bis(2-ethylhexyl)amine (5.5 g, 22.9 mmol), and CH_2Cl_2 (100 mL) were added to a 250 mL round-bottomed flask. The reaction mixture was stirred for 12 h under N_2 atmosphere, then the reaction mixture was filtered and the residue was washed with CH_2Cl_2. The filtrate was concentrated under reduced pressure. The crude product was subjected to column chromatography (4/1, *v*/*v*, *n*-hexane/ethyl acetate on silica, $R_f \approx 0.48$) affording the compound 1-A as a colorless oil (7.9 g, yield 80%). ^{1}H NMR ($CDCl_3$, 400 MHz, ppm): δ 4.16 (s, 2H), 3.18 (t, *J*=20.2 Hz, 4H), 2.66 (d, *J*=36.3 Hz, 3H), 1.76-1.53 (m, 6H), 1.44 (s, 9H), 1.23 (d, *J*=20.9 Hz, 16H), 0.92-0.82 (m, 12H). ^{13}C NMR ($CDCl_3$, 101 MHz, ppm): δ 175.10, 154.71, 79.54, 51.32, 49.10, 39.24, 39.09, 37.13, 30.61, 28.89, 28.75, 28.68, 28.49, 23.90, 23.13, 23.07, 14.12, 14.09, 11.02, 10.73.

2.2.2. Synthesis of 1-(3,5-dihydroxyphenyl)-*N*,*N*-bis(2-ethylhexyl)piperidine-4-carboxamide (1-B)

Compound 1-A (5.4 g, 11.9 mmol) was dissolved in CH_2Cl_2 and cooled to 0°C. Trifluoroacetic acid (TFA) was added and the solution was allowed to warm to room temperature. After stirring at room

temperature until starting material was consumed (TLC monitoring), the solution was poured into water, neutralized with NaOH solution, and extracted with CH_2Cl_2. The combined organic layer was dried over $MgSO_4$, filtered, and concentrated to give a colorless oil in quantitative yield that was used immediately in the next step. Then phloroglucinol (1.6 g, 13.0 mmol), 1-butanol (30 mL), and toluene (60 mL) were added and heated at reflux with a Dean-Stark apparatus for 8 h. During that time, the solution progressed from colorless to pale red. Excess solvent was removed under reduced pressure, and an obtained reddish oil was purified by column chromatography (1/1, *v*/*v*, *n*-hexane/ethyl acetate on silica, $R_f \approx 0.40$), affording the compound 1-B as a colorless solid (3.4 g, yield 62%). ^{1}H NMR (DMSO-d_6, 400 MHz, ppm): δ 8.87 (s, 2H), 5.79 (s, 2H), 5.71 (s, 1H), 3.58 (d, J=11.9 Hz, 2H), 3.25-3.14 (m, 4H), 2.65 (t, J=11.4 Hz, 3H), 1.70-1.53 (m, 6H), 1.29-1.16 (m, 16H), 0.84 (dd, J=23.8, 6.1 Hz, 12H). ^{13}C NMR (DMSO-d_6, 101 MHz, ppm): δ 174.94, 159.24, 153.23, 94.88, 94.36, 50.53, 48.72, 48.08, 38.83, 38.57, 36.81, 33.81, 30.38, 28.72, 28.56, 23.74, 23.00, 14.34, 11.28, 10.90.

2.2.3. Synthesis of 1-(3-(dodecyloxy)-5-hydroxyphenyl)-*N*,*N*-bis(2-ethylhexyl)-piperidine-4-carbox -amide (1-C)

Compound 1-B (2.3 g, 5.0 mmol), 1-bromododecane (1.2 g, 5.0 mmol), 18-crown-6 (0.13 g, 0.5 mmol), and K_2CO_3 (0.83 g, 6.0 mmol) were added in dry *N*,*N*-dimethylformamide (DMF, 50 mL). After stirring at room temperature for 12 h, the solution was poured into water and extracted three times by CH_2Cl_2. The combined organic phase was dried over anhydrous Na_2SO_4, concentrated in a vacuum, and purified by column chromatography on silica (3/1, *v*/*v*, *n*-hexane/ethyl acetate on silica, $R_f \approx 0.35$), affording the compound 1-C as a yellowish oil (1.5 g, yield 47%). ^{1}H NMR (500 MHz, $CDCl_3$, ppm): δ 7.51 (s, 1H), 6.17 (s, 1H), 5.97 (d, J=7.7 Hz, 2H), 3.85 (t, J=6.5 Hz, 2H), 3.68 (d, J=11.7 Hz, 2H), 3.23 (dd, J=49.7, 12.4 Hz, 4H), 2.62 (dt, J=23.4, 11.6 Hz, 3H), 2.03-1.96 (m, 2H), 1.76-1.65 (m, 6H), 1.57 (s, 2H), 1.26 (s, 32H), 0.88 (dd, J=12.3, 7.3 Hz, 15H). ^{13}C NMR (126 MHz, $CDCl_3$, ppm): δ 175.89, 160.97, 158.35, 153.43, 97.33, 95.36, 93.38, 67.84, 60.49, 51.27, 49.47, 49.24, 39.33, 39.15, 37.08,

31.94, 30.57, 30.48, 29.69, 29.66, 29.64, 29.62, 29.46, 29.37, 28.95, 28.80, 28.68, 26.11, 23.84, 23.80, 23.10, 23.02, 22.71, 21.05, 14.19, 14.13, 14.09, 14.06, 10.98, 10.72.

2.2.4. Synthesis of the fluorophore SQ1

A 100 mL round bottom flask, charged with the compound 1-C (1.3 g, 2.0 mmol) and squaric acid (0.11 g, 1.0 mmol) dissolved in a 1-butanol/toluene mixture (50 mL, 1/1, *v*/*v*). The resulting mixture was heated at reflux with a Dean-Stark apparatus for 8 h to generate a dark green solution. The reaction mixture was cooled down to room temperature and excess solvent was removed under reduced pressure. The crude mixture was purified by column chromatography (3/1, *v*/*v*, *n*-hexane/ethyl acetate on silica, $R_f \approx 0.43$) to afford SQ1 as a blue solid (0.77 g, yield 56%). ^{1}H NMR (500 MHz, $CDCl_3$, ppm): δ 14.16 (s, 2H), 5.90 (s, 2H), 5.73 (s, 2H), 3.99 (dd, *J*=14.7, 8.1 Hz, 8H), 3.27 (d, *J*=5.3 Hz, 4H), 3.17 (d, *J*=7.3 Hz, 4H), 3.07 (t, *J*=11.3 Hz, 4H), 2.79 (t, *J*=10.3 Hz, 2H), 1.94 (dt, *J*=19.8, 9.7 Hz, 8H), 1.79 (d, *J*=10.9 Hz, 4H), 1.67 (s, 2H), 1.57 (s, 2H), 1.43 (d, *J*=7.5 Hz, 4H), 1.25 (s, 64H), 0.89 (dt, *J*=17.3, 8.6 Hz, 30H). ^{13}C NMR (126 MHz, $CDCl_3$, ppm): δ 174.56, 166.60, 163.16, 158.07, 104.61, 95.06, 89.14, 69.29, 51.34, 48.99, 46.65, 39.11, 38.11, 37.06, 31.95, 30.58, 30.54, 29.71, 29.69, 29.67, 29.64, 29.43, 29.39, 28.86, 28.69, 28.35, 26.15, 23.85, 23.10, 23.04, 22.71, 14.15, 14.09, 14.07, 11.01, 10.68. HRMS (APCI, [M+H$^+$], *m*/*z*): calculated for $C_{84}H_{143}N_4O_8^+$: 1336.0900, found: 1336.0914.

2.3. Synthesis of the fluorophore SQ2

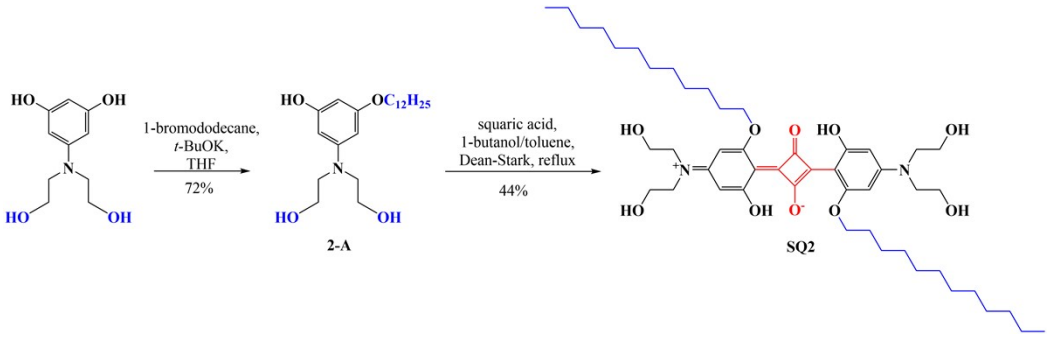

Scheme S2. Synthesis route for the fluorophore SQ2.

The synthesis details of SQ2 were presented in Scheme S2. Synthesis of 5-(bis(2-hydroxyethyl)amino)benzene-1,3-diol was performed based on the previously reported literatures.[9,10]

^{1}H NMR (DMSO-d_6, 400 MHz, ppm): δ 8.77 (s, 2H), 5.57 (s, 2H), 5.52 (s, 1H), 4.74 (s, 2H), 3.49 (s, 4H), 3.28 (t, J=6.2 Hz, 4H).

2.3.1. Synthesis of compound 2-A

5-(bis(2-hydroxyethyl)amino)benzene-1,3-diol (1.7 g, 8.0 mmol), 1-bromododecane (2.2 g, 8.8 mmol), 18-crown-6 (0.2 g, 0.8 mmol), and potassium *tert*-butoxide (1.1 g, 9.6 mmol) were added to 50 mL dry THF. After stirring at room temperature for 12 h, the solution was concentrated before water was added. The aqueous solution was extracted three times by CH_2Cl_2. The combined organic phase was dried over anhydrous Na_2SO_4, concentrated in a vacuum, and purified by column chromatography (ethyl acetate on silica, $R_f \approx 0.38$), affording the compound 2-A as a pale solid (2.2 g, yield 72%). ^{1}H NMR (DMSO-d_6, 500 MHz, ppm): δ 8.94 (s, 1H), 5.70 (s, 1H), 5.65 (s, 1H), 5.62 (s, 1H), 4.74 (t, J=5.4 Hz, 2H), 3.81 (t, J=6.4 Hz, 2H), 3.49 (s, 4H), 3.31 (t, J=6.5 Hz, 4H), 1.69-1.60 (m, 2H), 1.25 (s, 18H), 0.86 (t, J=6.8 Hz, 3H). ^{13}C NMR (DMSO-d_6, 126 MHz, ppm): δ 161.15, 159.47, 150.10, 92.13, 90.40, 90.05, 67.34, 58.67, 53.88, 31.77, 29.49, 29.29, 29.19, 22.57, 14.42.

2.3.2. Synthesis of the fluorophore SQ2

SQ2 was synthesized in the same reaction conditions as SQ1. The crude product was subjected to column chromatography (6/2/1, *v*/*v*/*v*, CH_2Cl_2/ethyl acetate/methanol on silica, $R_f \approx 0.63$) affording SQ2 as a green solid (yield 44%). ^{1}H NMR (DMSO-d_6, 500 MHz, ppm): δ 13.57 (s, 2H), 5.85 (s, 2H), 5.81 (s, 2H), 4.92 (s, 4H), 3.99 (s, 4H), 3.59 (s, 16H), 1.81 (s, 4H), 1.22 (d, J=14.8 Hz, 36H), 0.84 (t, J=6.1 Hz, 6H). ^{13}C NMR (DMSO-d_6, 126 MHz, ppm): δ 181.21, 170.85, 164.99, 162.32, 157.71, 103.08, 94.00, 89.43, 68.90, 59.01, 54.05, 31.80, 29.54, 29.46, 29.22, 22.58, 14.42. HRMS (APCI, [M+H$^+$], *m*/*z*): calculated for $C_{48}H_{77}N_2O_{10}^+$: 841.5573, found: 841.5573.

3. Comparative spectral emission region of some commercial fluorophores

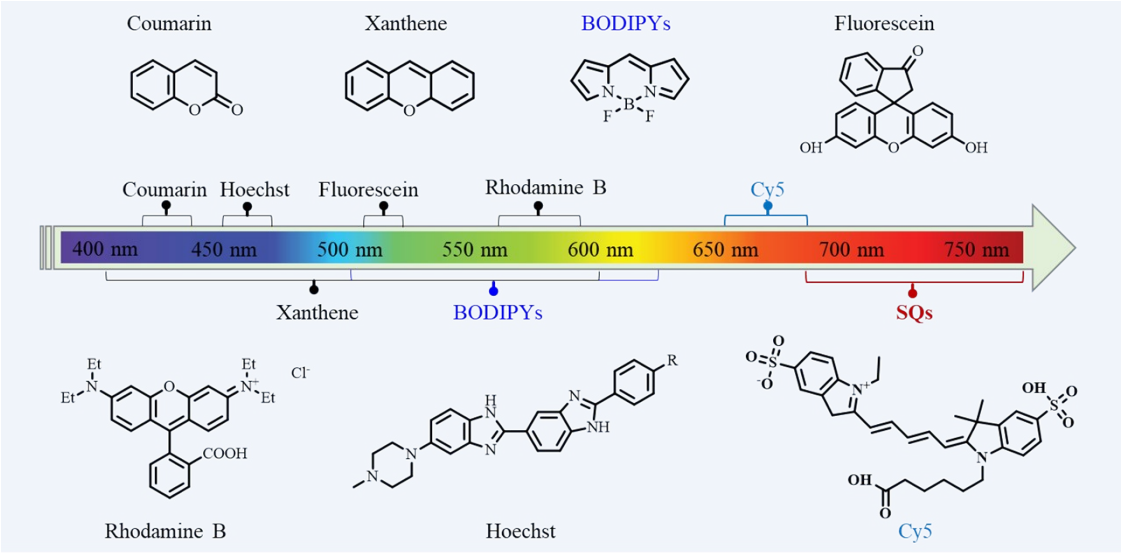

Scheme S3. Comparative spectral emission region of some commercial fluorophores.

4. Linear photophysical properties

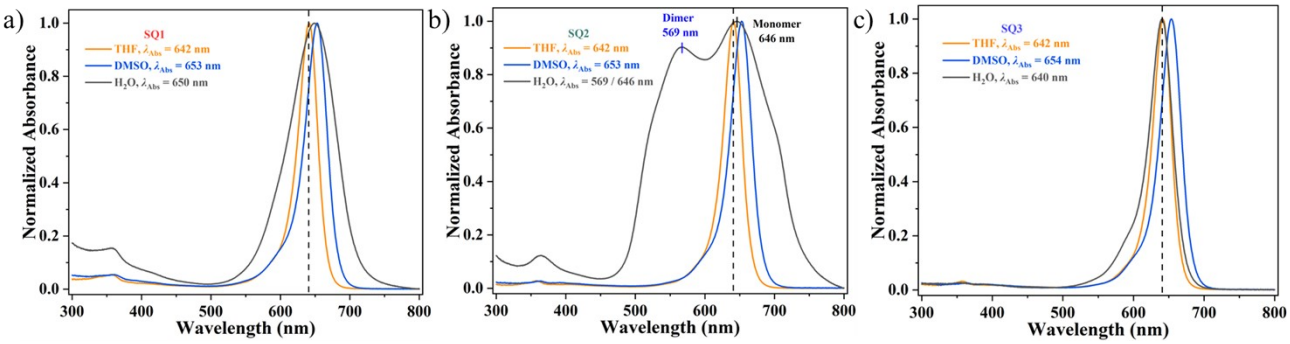

Fig. S1. Combined UV-vis absorption spectra of the fluorophores SQ1 (a), SQ2 (b), and SQ3 (c) in different solvents including THF, DMSO, and H_2O.

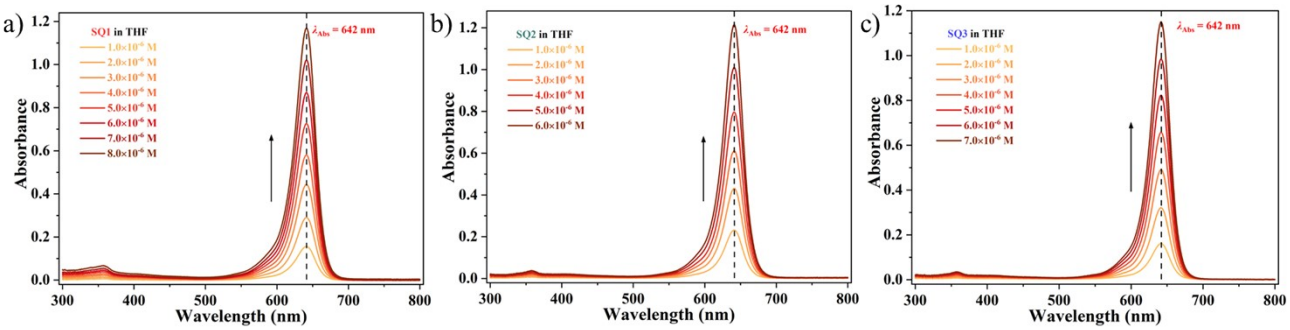

Fig. S2. Concentration effect of the fluorophores SQ1 (a), SQ2 (b), and SQ3 (c) in THF.

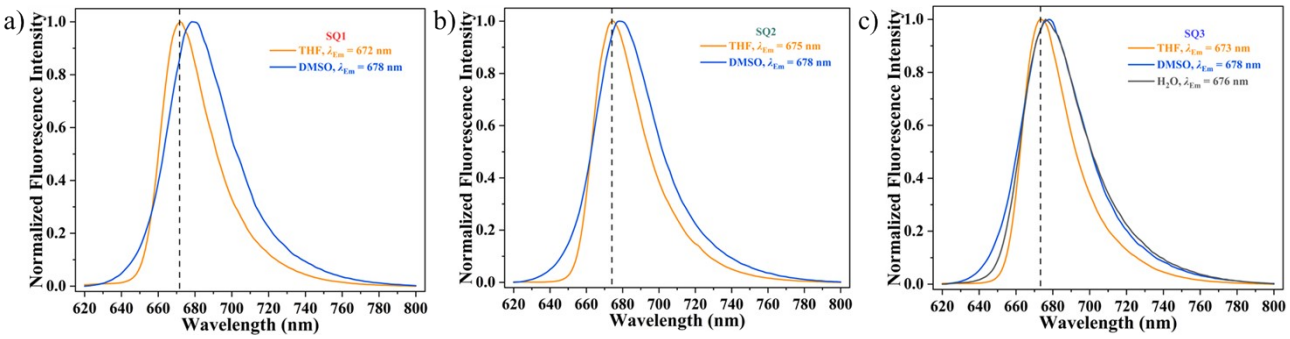

Fig. S3. Normalized fluorescence spectra of the fluorophores SQ1 (a), SQ2 (b), and SQ3 (c) in different solvents including THF, DMSO, and H_2O.

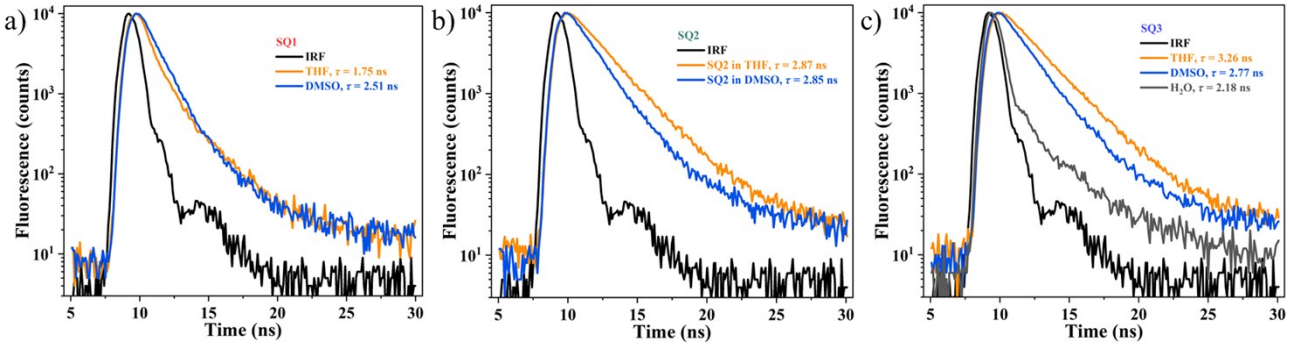

Fig. S4. Fluorescence lifetime decay traces of the fluorophores SQ1 (a), SQ2 (b), and SQ3 (c) recorded in different solvents including THF, DMSO, and H_2O.

5. Two-photon absorption (2PA) and two-photon excited fluorescence (2PEF) properties

Table S1. 2PA cross section (δ_{2PA}) values of the SQs and the reference RDB[11] in THF ranging from 750 to 870 nm.

Comp.	750 nm	760 nm	770 nm	780 nm	790 nm	800 nm	810 nm	820 nm	830 nm	840 nm	870 nm
SQ1	1110 GM	784 GM	535 GM	612 GM	594 GM	776 GM	912 GM	991 GM	677 GM	477 GM	175 GM
SQ2	1100 GM	731 GM	679 GM	801 GM	955 GM	1060 GM	1010 GM	991 GM	633 GM	357 GM	315 GM
SQ3	886 GM	723 GM	727 GM	785 GM	755 GM	1220 GM	991 GM	799 GM	757 GM	490 GM	33 GM
RDB	48 GM	53 GM	67 GM	95 GM	94 GM	102 GM	122 GM	97 GM	125 GM	145 GM	80 GM

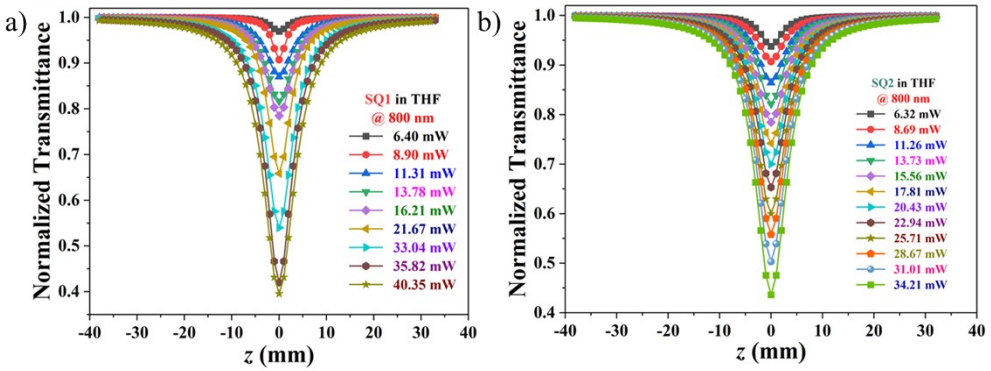

Fig. S5. Normalized transmittance curves of SQ1 (a) and SQ2 (b) in THF excited at fs-800 nm under various laser input intensities.

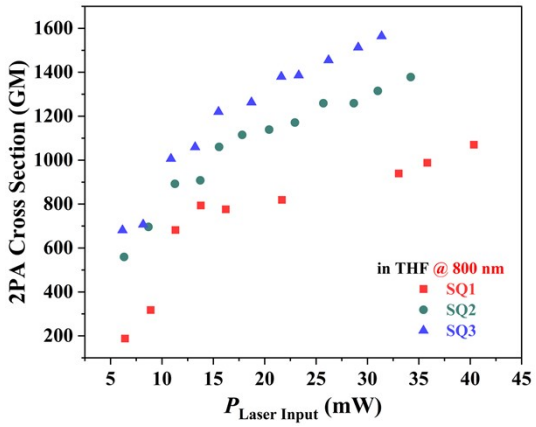

Fig. S6. 2PA cross section (δ_{2PA}) values of the three SQs in THF measured at fs-800 nm as a function of input laser power at the focal plane.

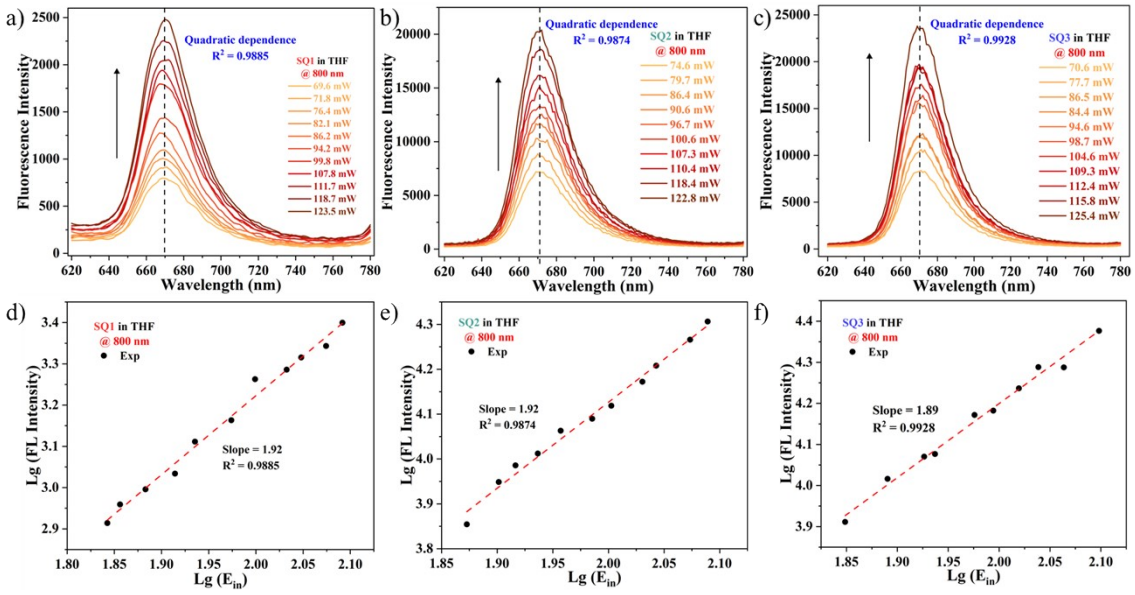

Fig. S7. 2PEF spectra of SQ1 (a), SQ2 (b), and SQ3 (c) in THF at various laser input values (λ_{ex} = fs-800 nm). Linear correlation plot of 2PEF intensity versus the excitation intensity for SQ1 (d), SQ2 (e), and SQ3 (f) in THF.

6. Confocal laser scanning microscope (CLSM) images of the onion epidermal cells

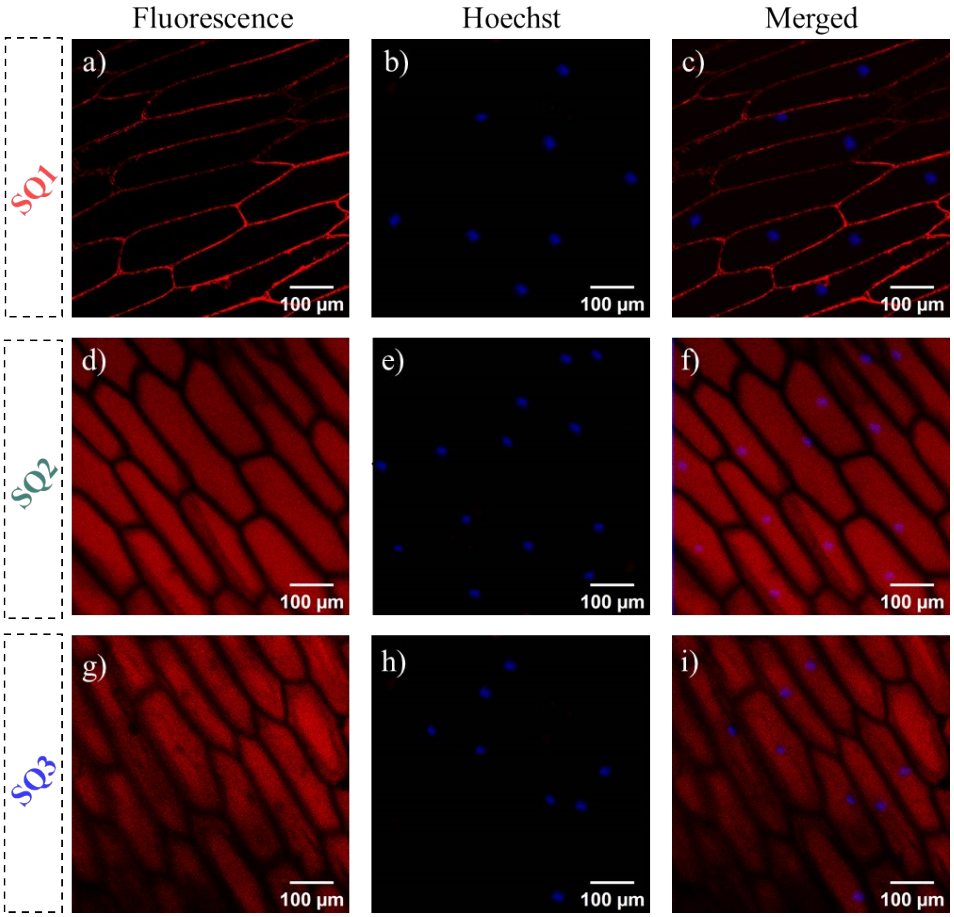

Fig. S8. CLSM images of the onion epidermal cells incubated with SQ1 (a), SQ2 (d), SQ3 (g), and Hoechst 33342 (b, e, h). Specifically, merged fluorescence (c, f, i) images of the SQs and Hoechst 33342.

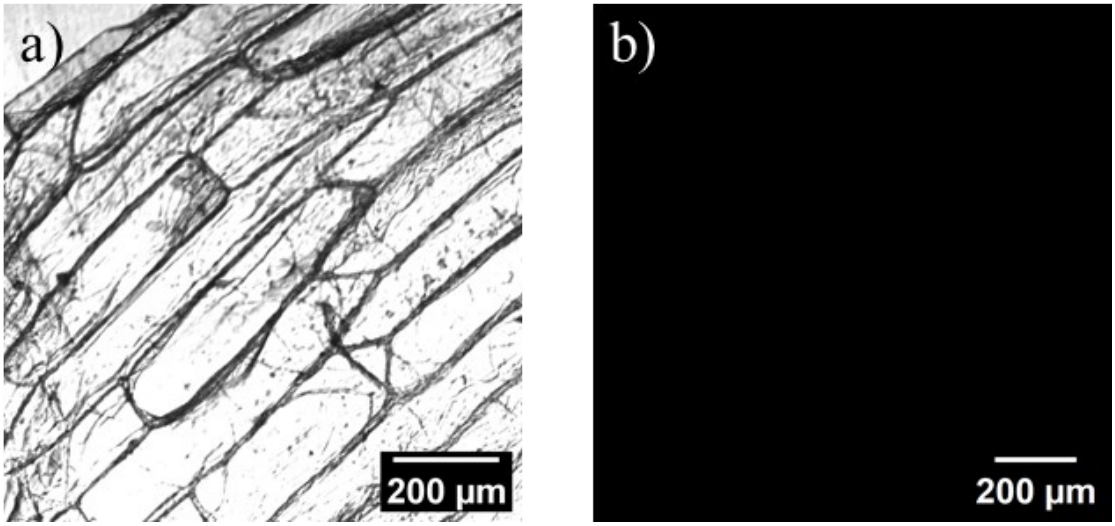

Fig. S9. Brightfield (a) and fluorescence (b, λ_{ex} = 635 nm) images of the original onion epidermal cell as a control.

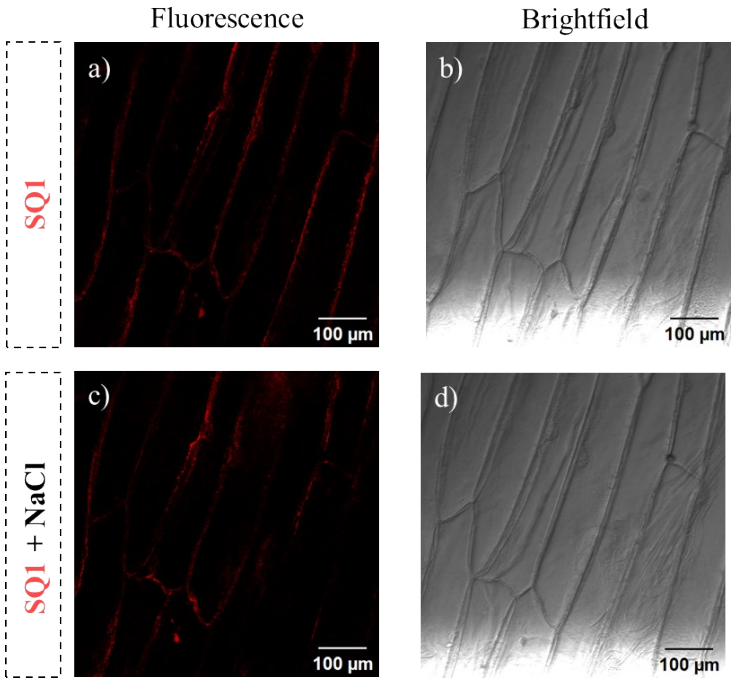

Fig. S10. Fluorescence (a) and brightfield (b) images of the onion epidermal cells stained with SQ1. Fluorescence (c) and brightfield (d) images of the onion epidermal cells stained with SQ1 co-existed with 20% NaCl solution. Notes: λ_{ex} = 635 nm.

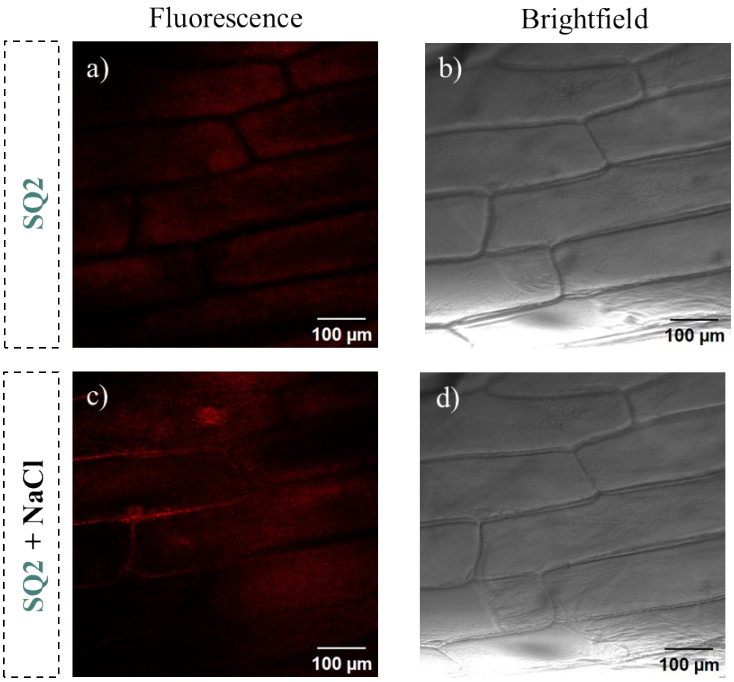

Fig. S11. Fluorescence (a) and brightfield (b) images of the onion epidermal cells stained with SQ2. Fluorescence (c) and brightfield (d) images of the onion epidermal cells stained with SQ2 co-existed with 20% NaCl solution. Notes: λ_{ex} = 635 nm.

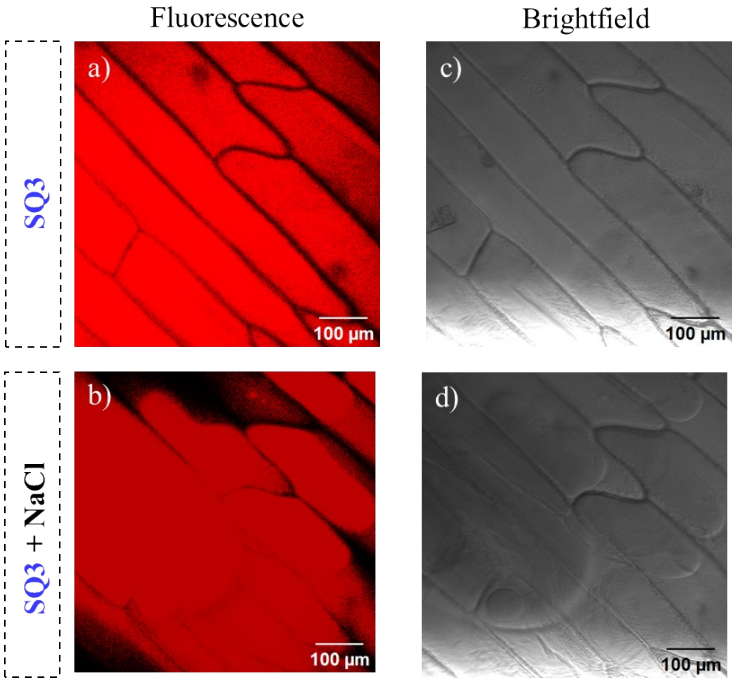

Fig. S12. Fluorescence (a) and brightfield (b) images of the onion epidermal cells stained with SQ3. Fluorescence (c) and brightfield (d) images of the onion epidermal cells stained with SQ3 co-existed with 20% NaCl solution. Notes: λ_{ex} = 635 nm.

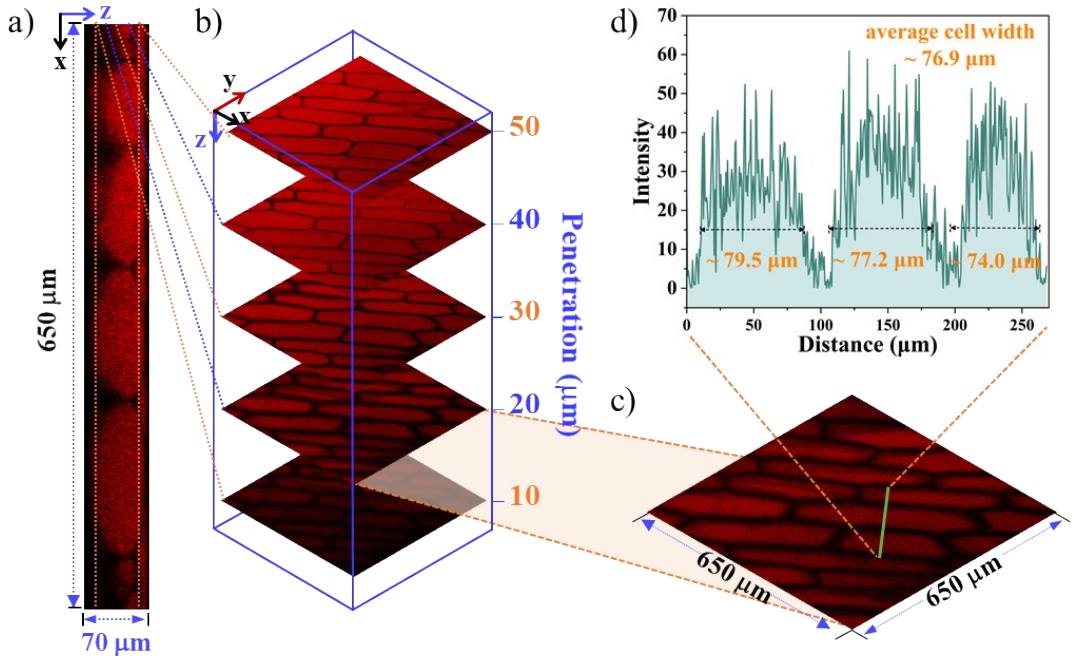

Fig. S13. (a) Cross-sectional (*x*-*z*) images of the onion epidermal cells. (b) Confocal *Z*-scan sections at different penetration depths of the onion epidermal cells incubated with SQ2. (c) 2D images of the onion epidermal cells at the specific depth of 20 μm. (d) Fluorescence intensity profiles of the onion epidermal cells. Notes: λ_{ex} = 635 nm.

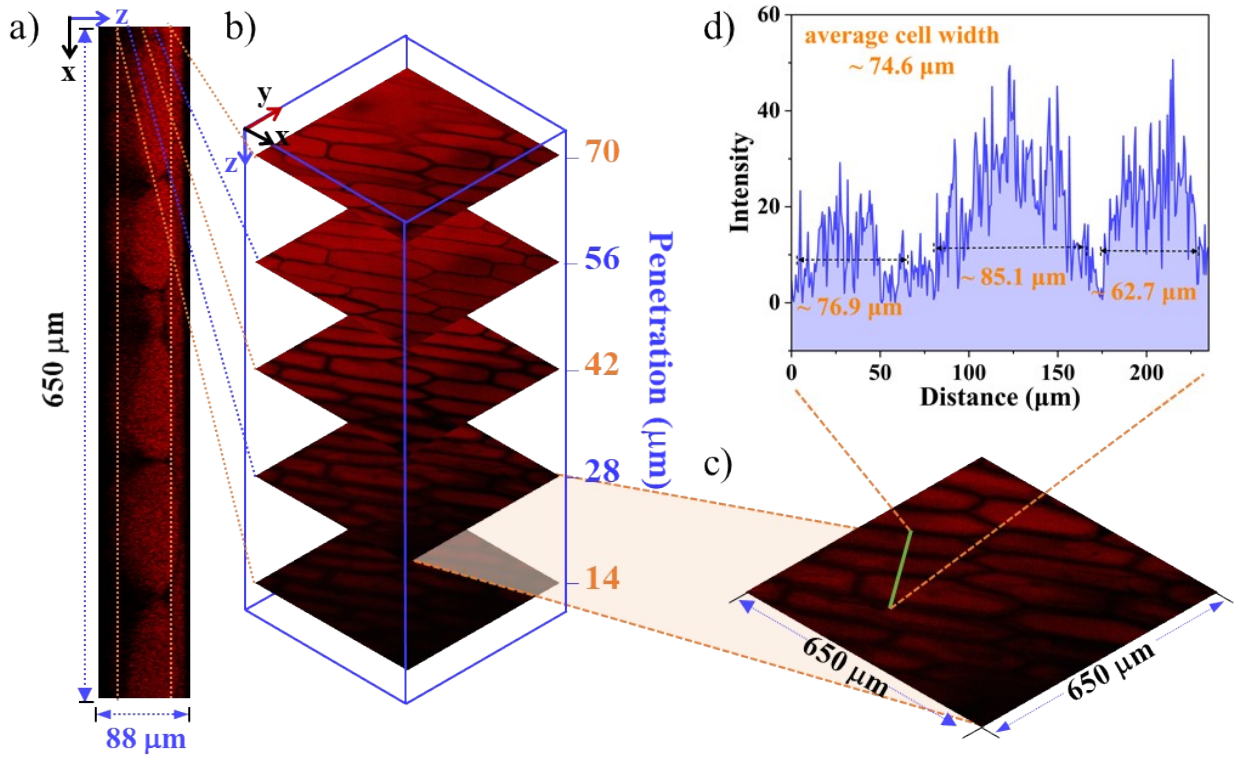

Fig. S14. (a) Cross-sectional (*x*-*z*) images of the onion epidermal cells. (b) Confocal *Z*-scan sections at different penetration depths of the onion epidermal cells incubated with SQ3. (c) 2D images of the onion epidermal cells at the specific depth of 28 µm. (d) Fluorescence intensity profiles of the onion epidermal cells. Notes: λ_{ex} = 635 nm.

7. *In vivo* images of the onion

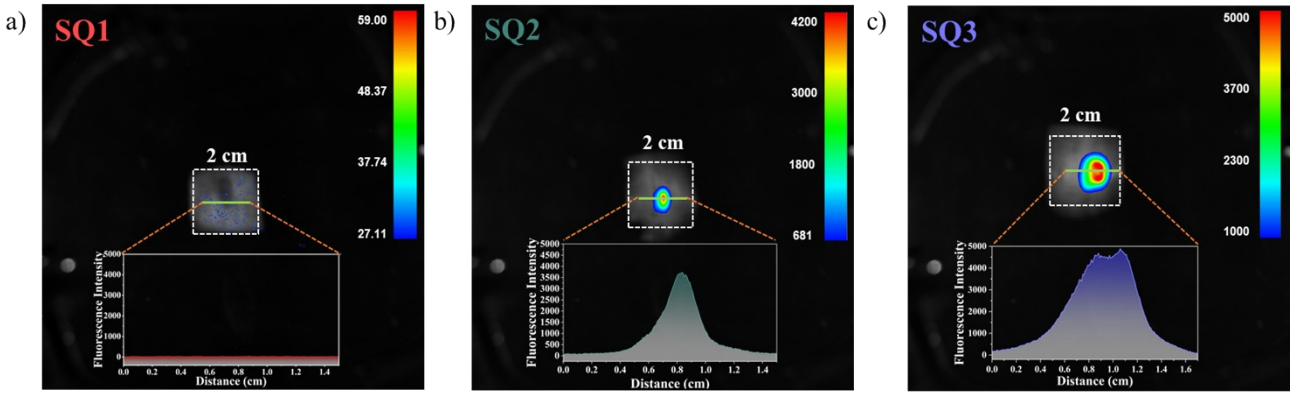

Fig. S15. *In vivo* images of SQ1 (a), SQ2 (b), and SQ3 (c) in onion (λ_{ex} = 650 nm). Insets showed the spectral intensities across the selected zone.

8. Confocal laser scanning microscope (CLSM) images of the Arabidopsis seedlings

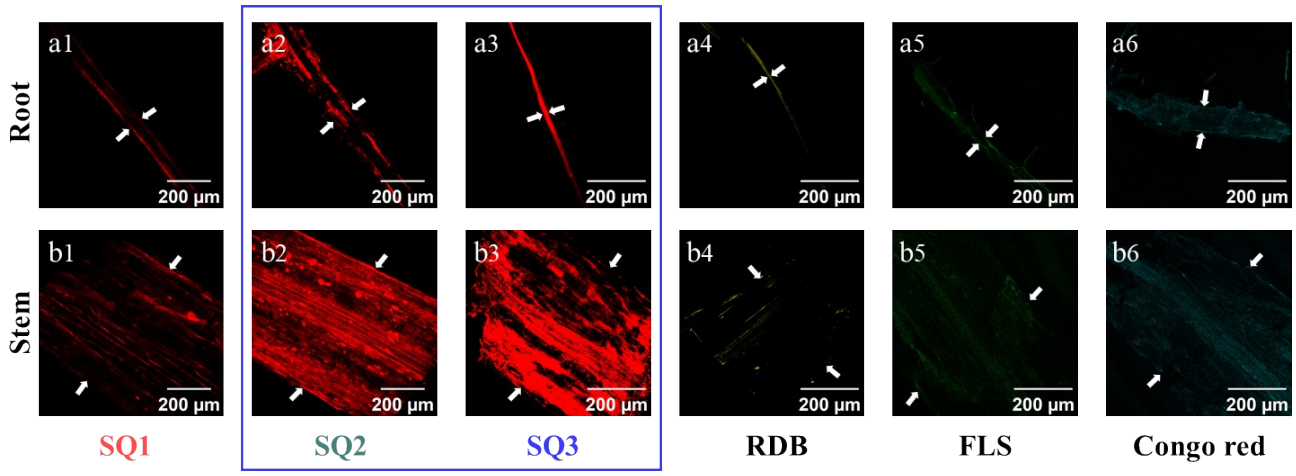

Fig. S16. Comparative CLSM images of the SQs and commercial fluorophores (RDB, FLS, and congo red; $c \sim 1.0 \times 10^{-4}$ mol/L) in the roots (a1 ~ a6) and stems (b1 ~ b6) of the Arabidopsis seedlings (10 min incubation; SQs: $\lambda_{ex} = 635$ nm; RDB: $\lambda_{ex} = 488$ nm; FLS: $\lambda_{ex} = 460$ nm; congo red: $\lambda_{ex} = 500$ nm).

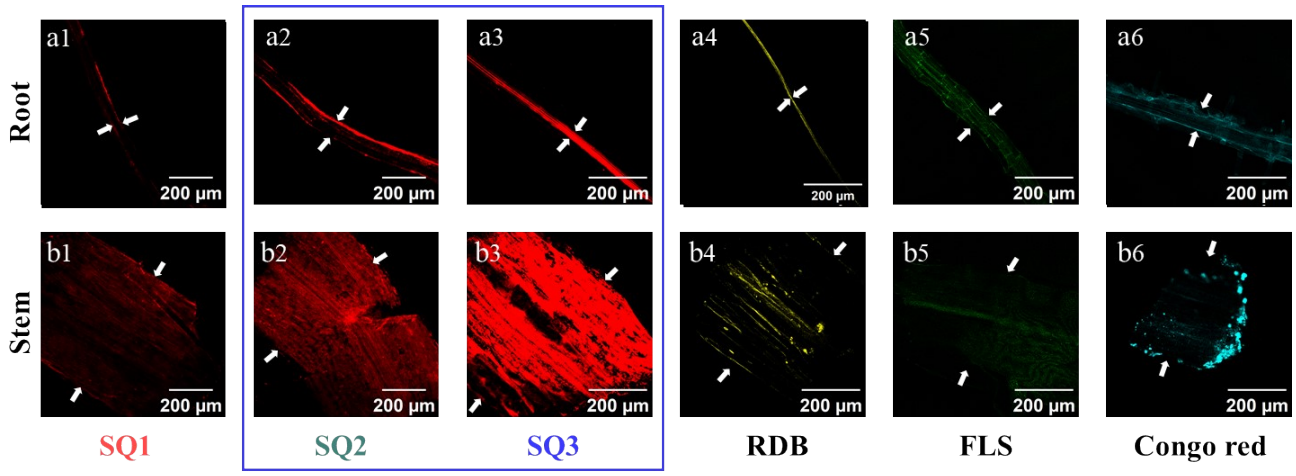

Fig. S17. Comparative CLSM images of the SQs and commercial fluorophores (RDB, FLS, and congo red; $c \sim 1.0 \times 10^{-4}$ mol/L) in the roots (a1 ~ a6) and stems (b1 ~ b6) of the Arabidopsis seedlings (30 min incubation; SQs: $\lambda_{ex} = 635$ nm; RDB: $\lambda_{ex} = 488$ nm; FLS: $\lambda_{ex} = 460$ nm; congo red: $\lambda_{ex} = 500$ nm).

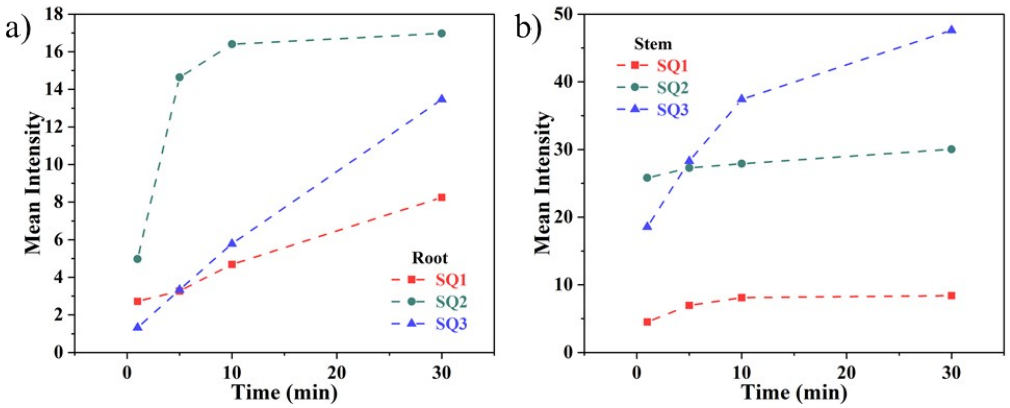

Fig. S18. Mean intensities of the roots (a) and stems (b) cultured with the SQs along with different incubation time (1, 5, 10, and 30 min).

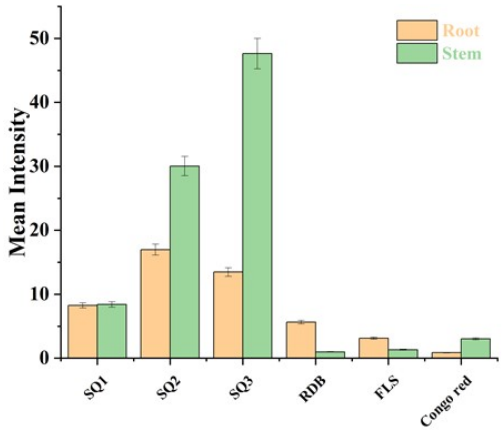

Fig. S19. Intensity comparison of the roots and stems cultured with different fluorophores under 5 min incubation.

9. Two-photon fluorescence microscope (2PFM) images

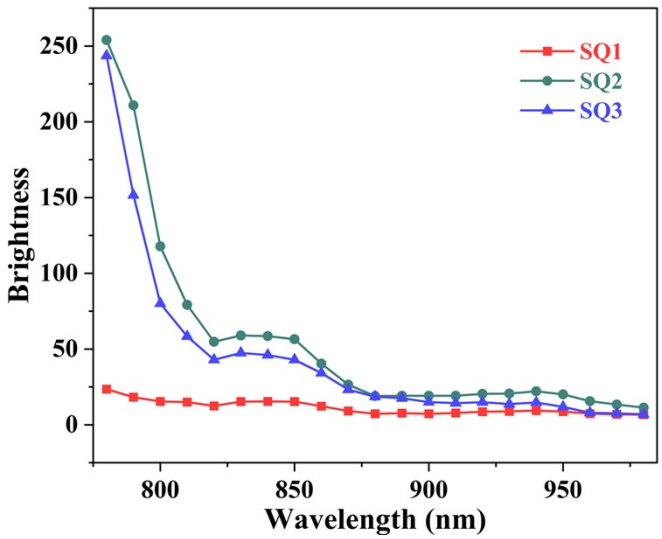

Fig. S20. Brightness of the SQs under two-photon excitation ranging from 760 to 980 nm.

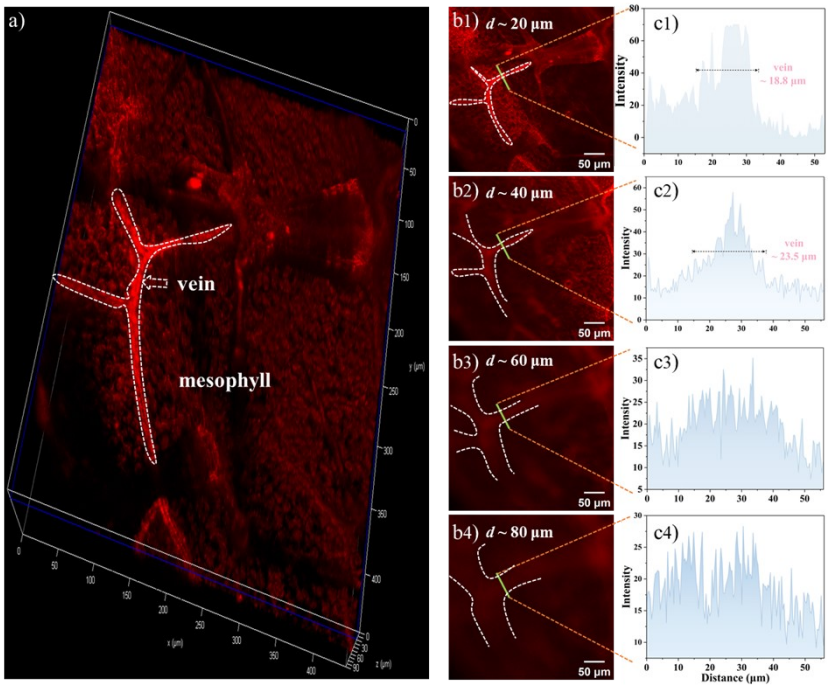

Fig. S21. (a) 3D 2PFM image of the Arabidopsis leaf incubated with SQ3. (b) Specific image of the leaf orthoslice at the selected penetration depths including 20 μm (b1), 40 μm (b2), 60 μm (b3), and 80 μm (b4). (c) Distribution histograms generated from the fluorescence intensity.

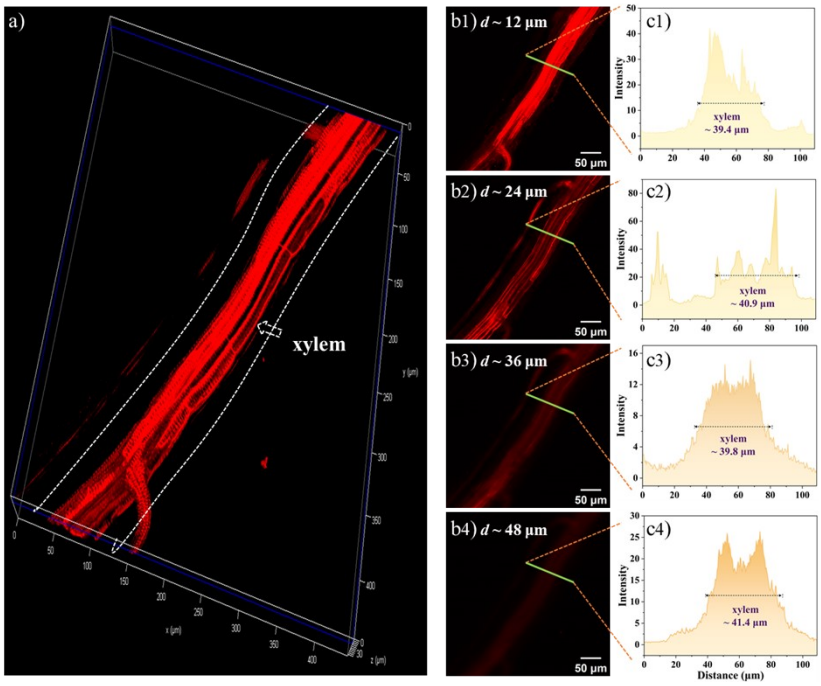

Fig. S22. (a) 3D 2PFM image of the Arabidopsis root incubated with SQ3. (b) Specific image of the root orthoslice at the selected penetration depths including 12 μm (b1), 24 μm (b2), 36 μm (b3), and 48 μm (b4). (c) Distribution histograms generated from the fluorescence intensity.

10. NMR spectra of the compounds

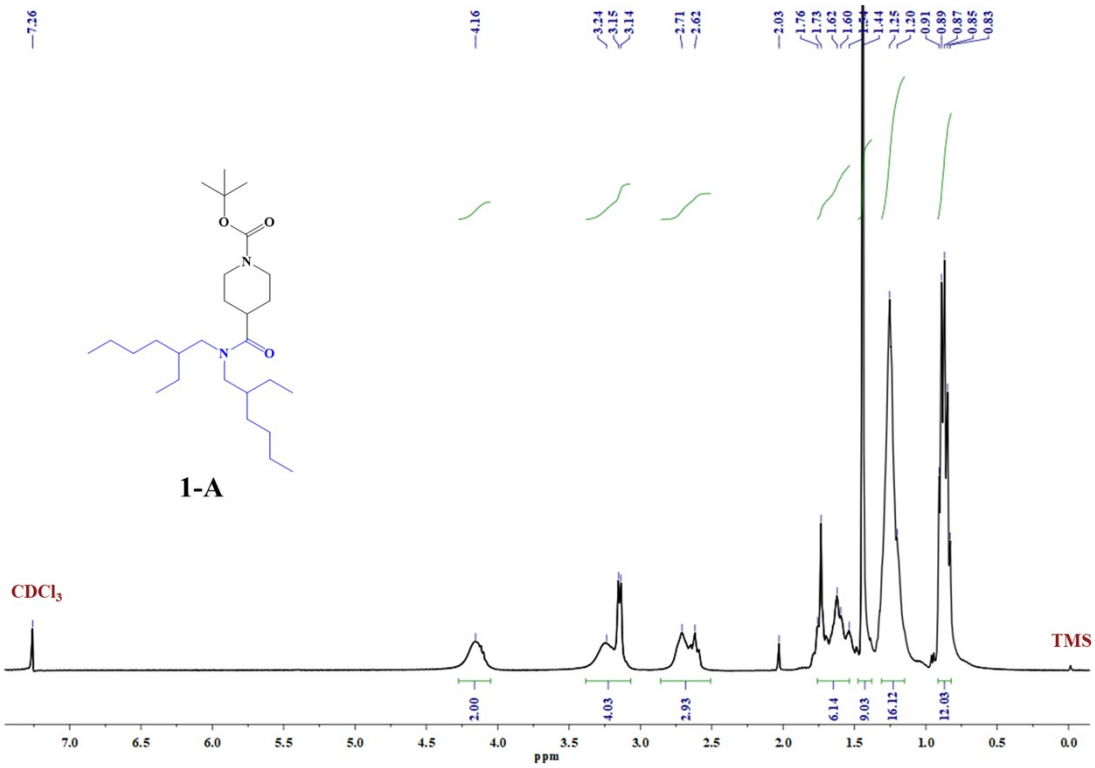

Fig. S23. ^{1}H NMR spectrum of the compound 1-A in $CDCl_3$.

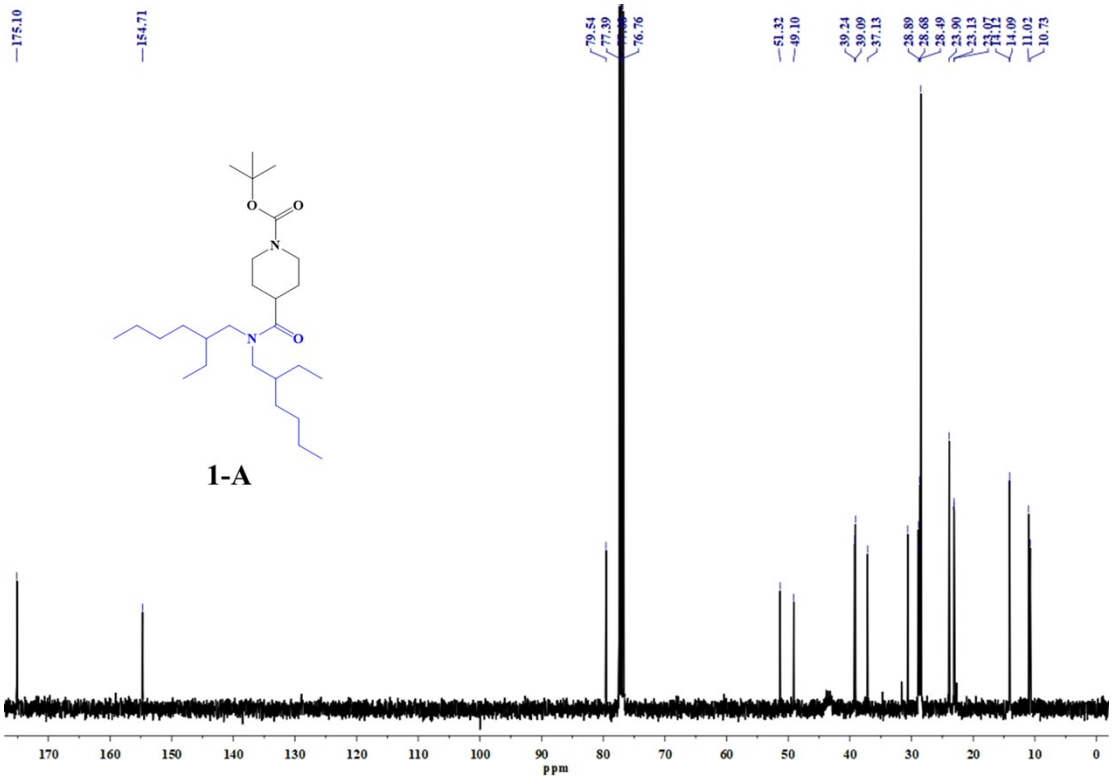

Fig. S24. ^{13}C NMR spectrum of the compound 1-A in $CDCl_3$.

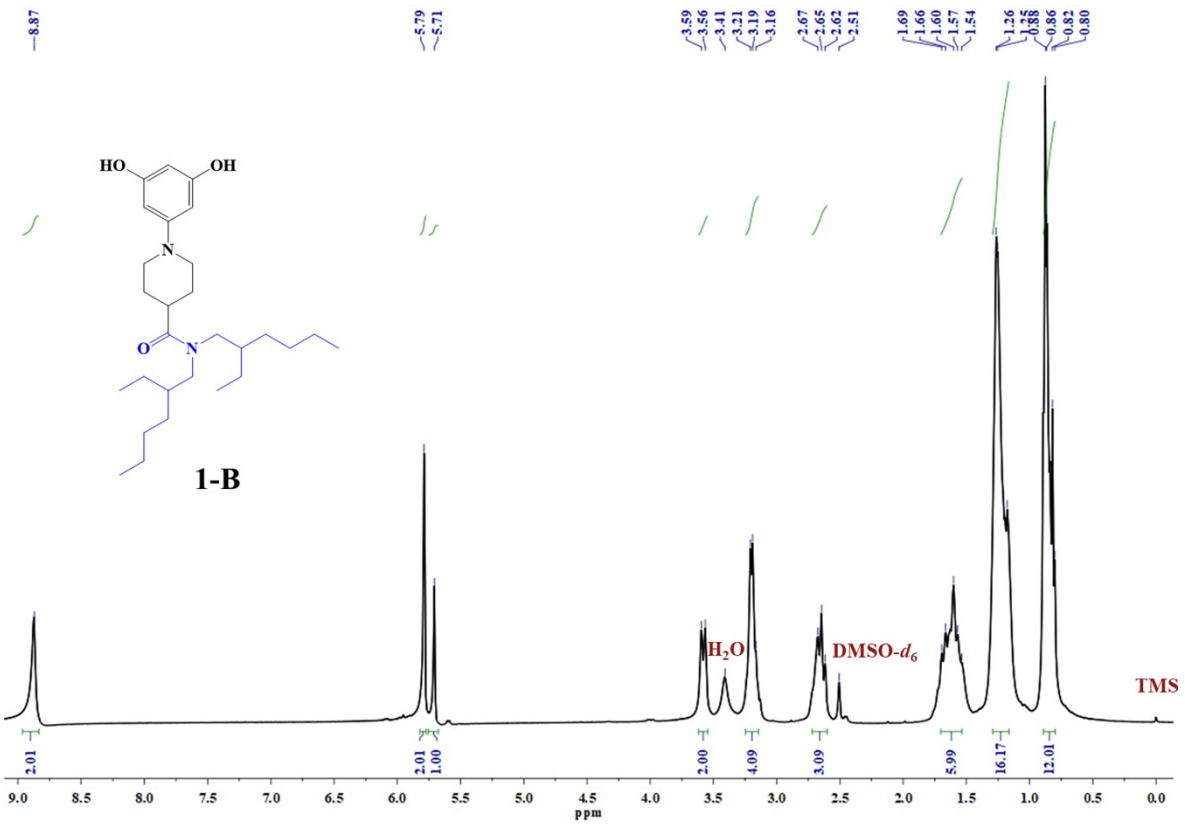

Fig. S25. ^{1}H NMR spectrum of the compound 1-B in DMSO-d_6.

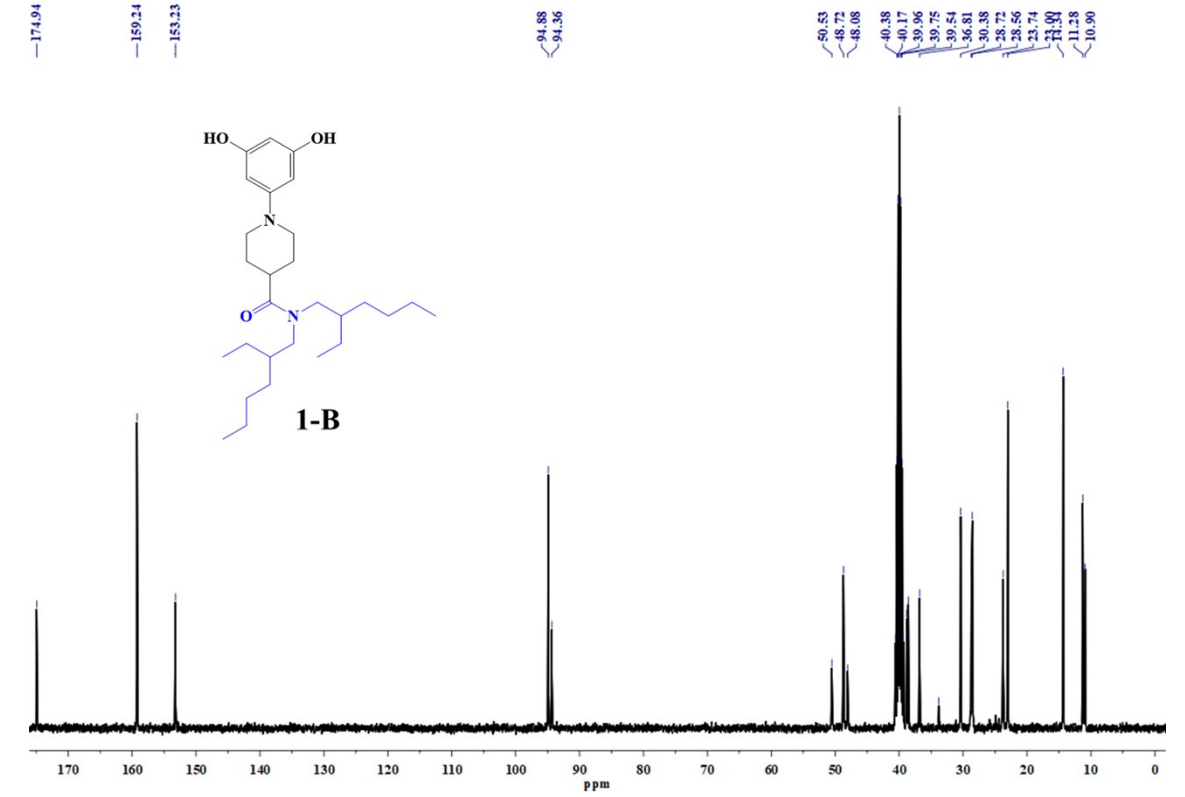

Fig. S26. ^{13}C NMR spectrum of the compound 1-B in DMSO-d_6.

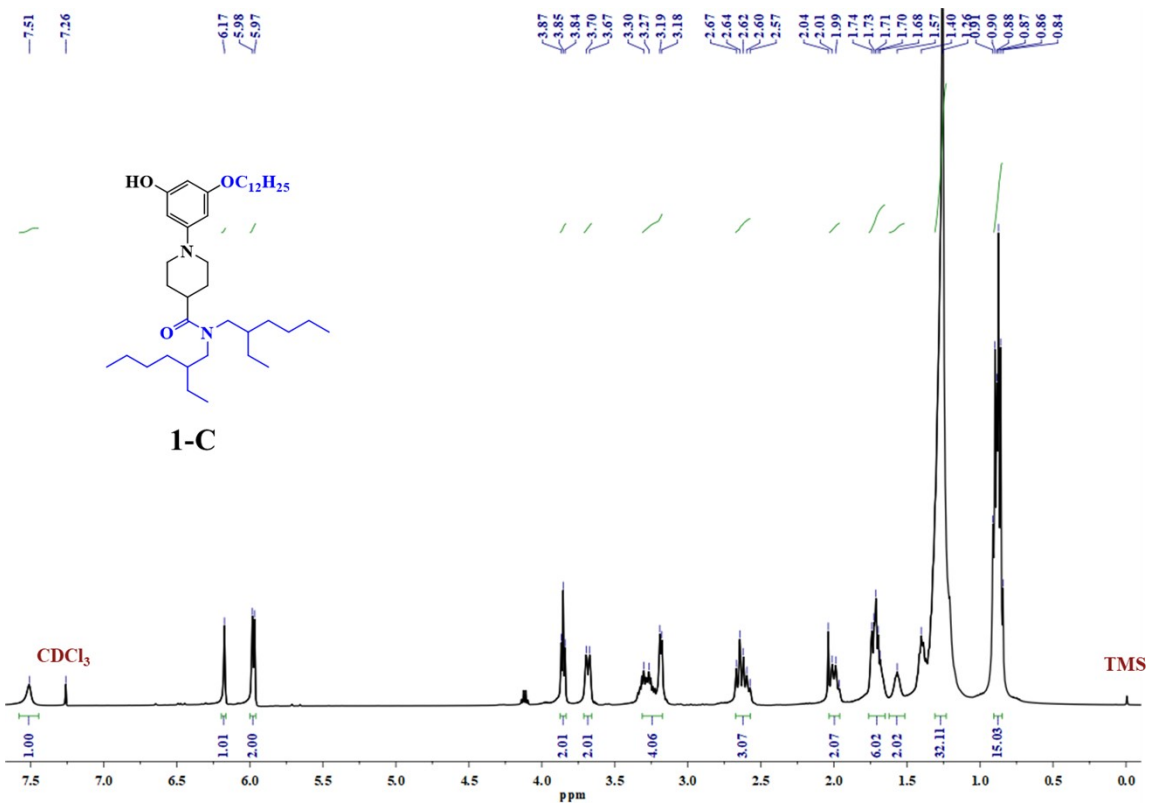

Fig. S27. ^{1}H NMR spectrum of the compound 1-C in $CDCl_3$.

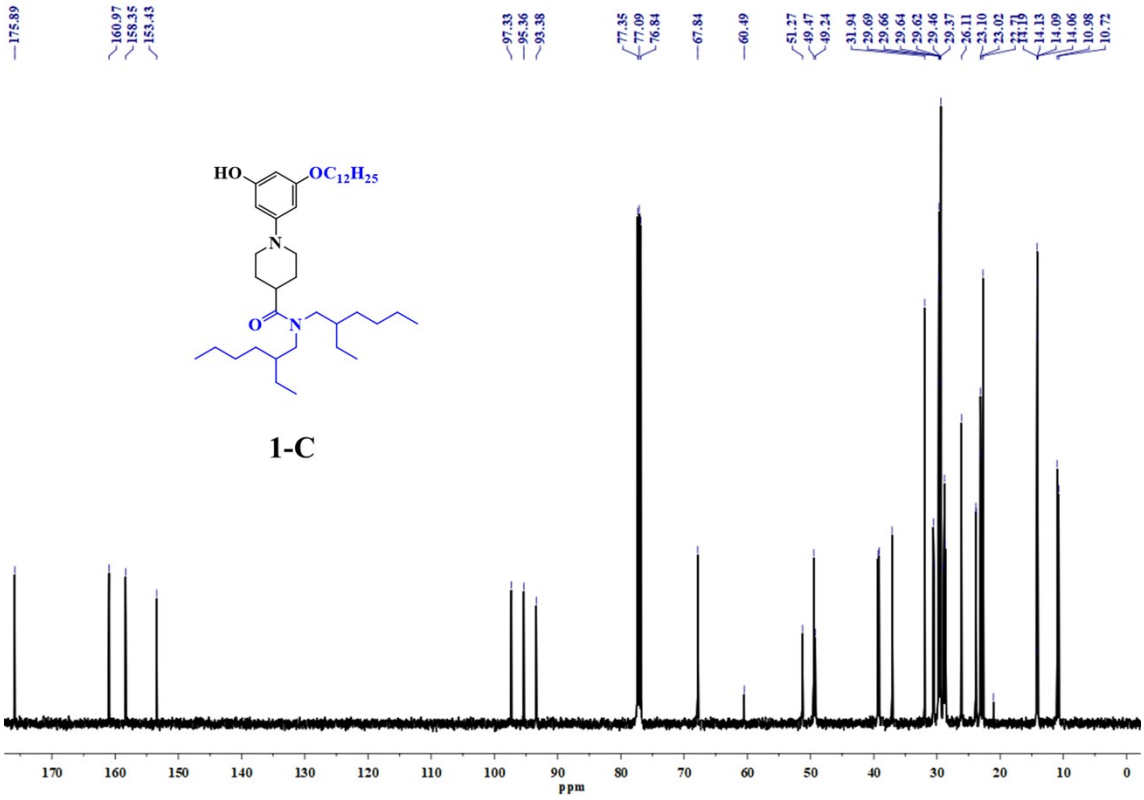

Fig. S28. ^{13}C NMR spectrum of the compound 1-C in $CDCl_3$.

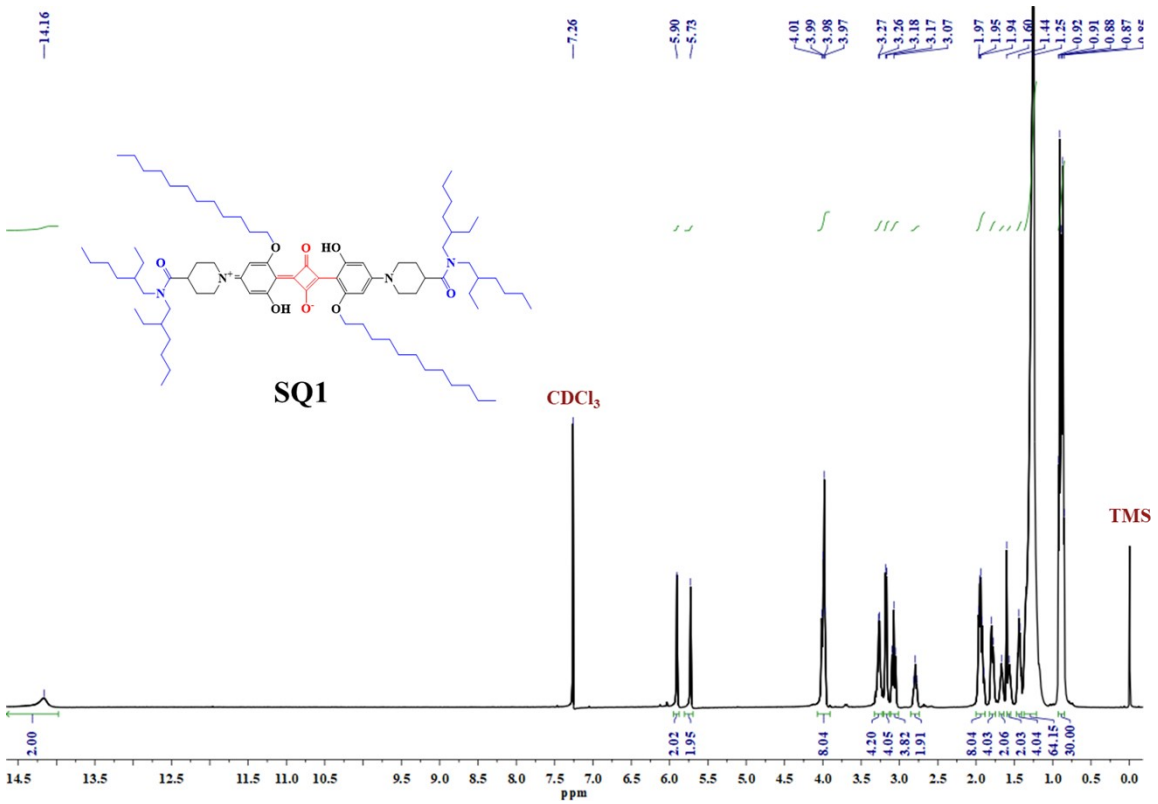

Fig. S29. ^{1}H NMR spectrum of the fluorophore SQ1 in $CDCl_3$.

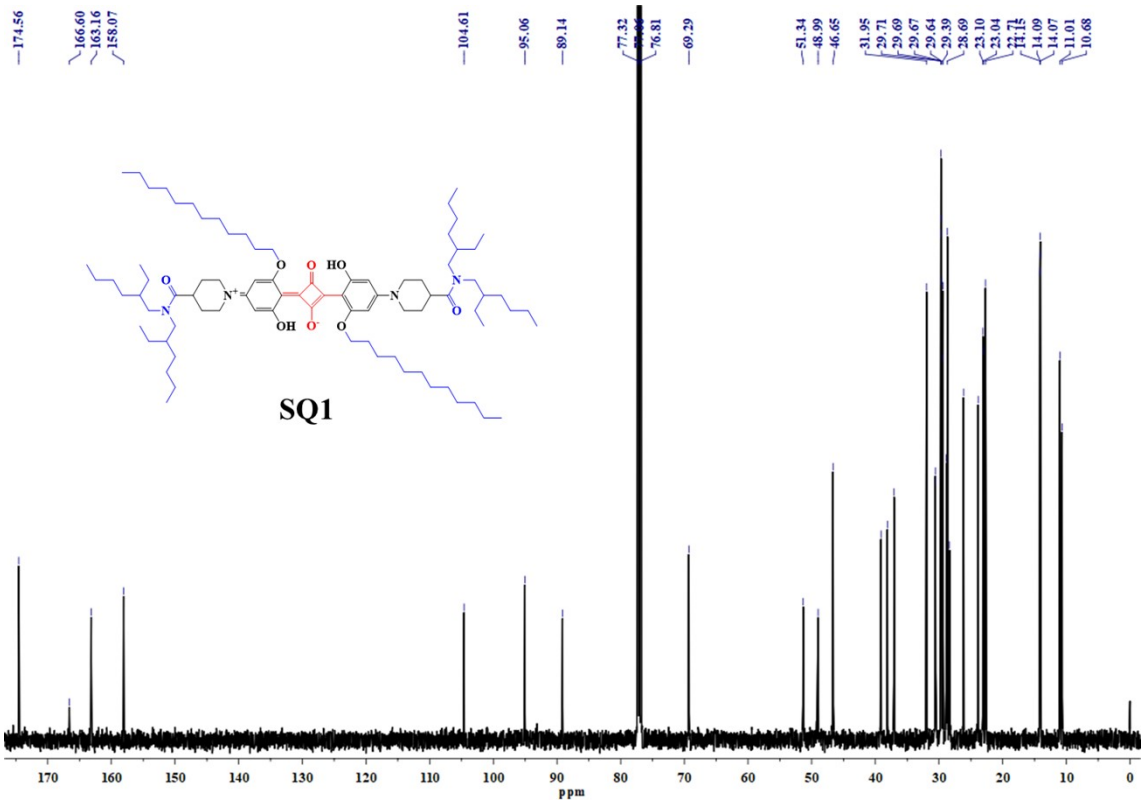

Fig. S30. ^{13}C NMR spectrum of the fluorophore SQ1 in $CDCl_3$.

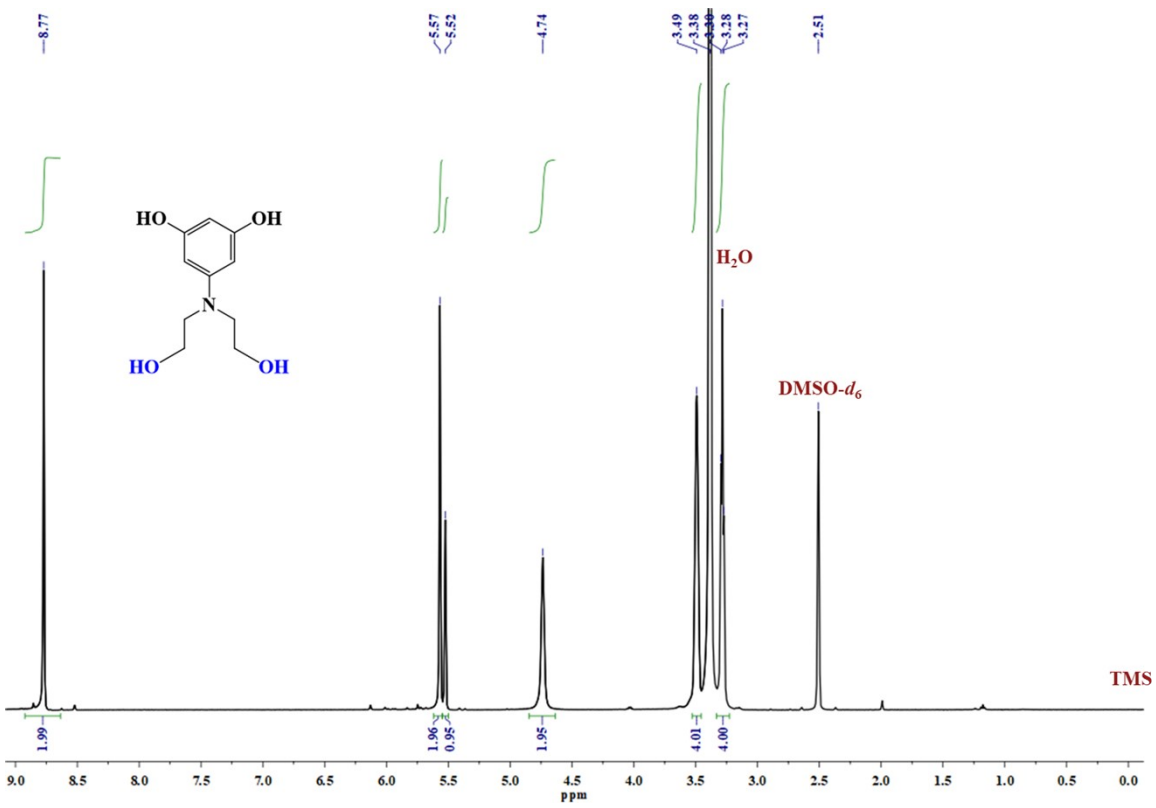

Fig. S31. ^{1}H NMR spectrum of the compound 5-(bis(2-hydroxyethyl)amino)benzene-1,3-diol in DMSO-d_6.

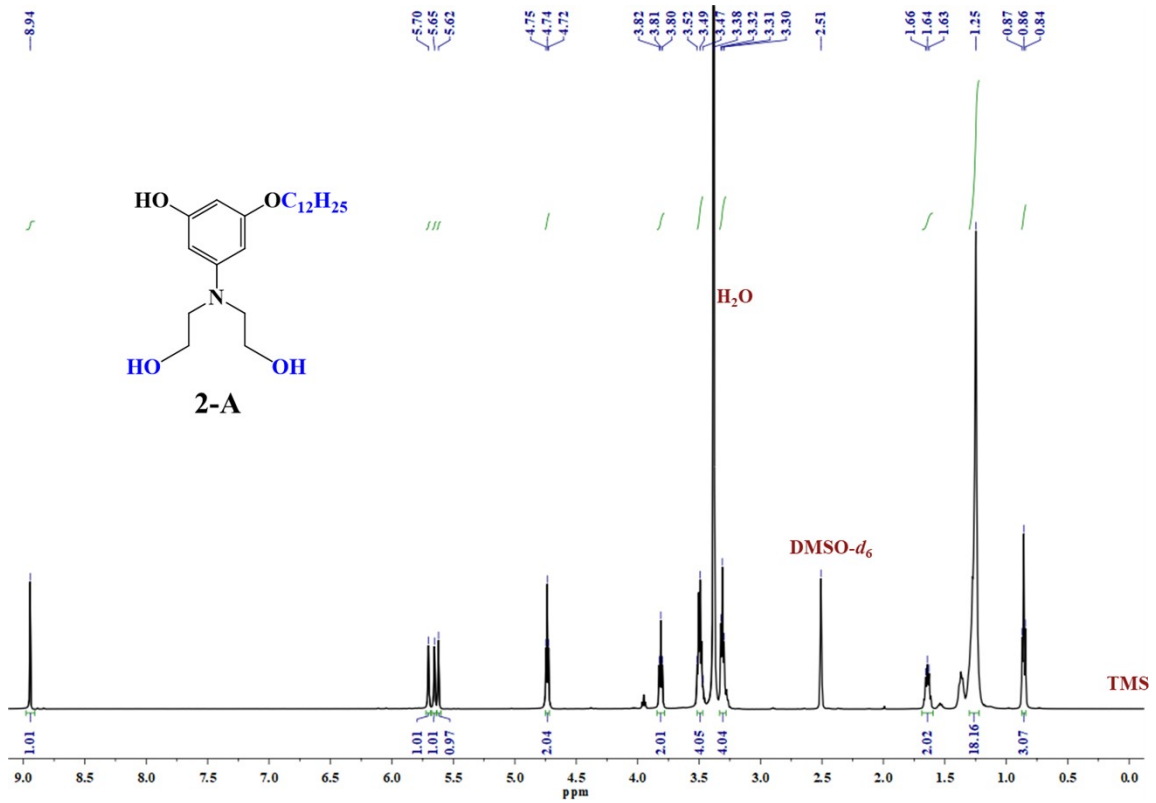

Fig. S32. ^{1}H NMR spectrum of the compound 2-A in DMSO-d_6.

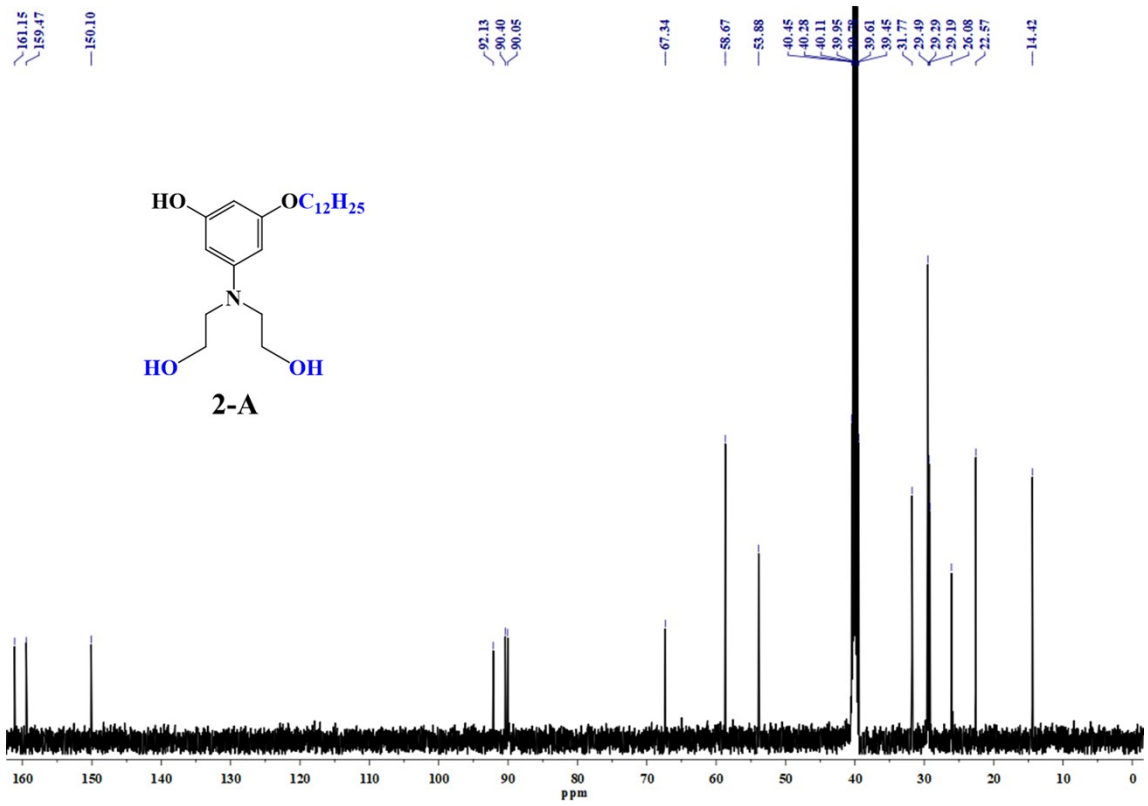

Fig. S33. ^{13}C NMR spectrum of the compound 2-A in DMSO-d_6.

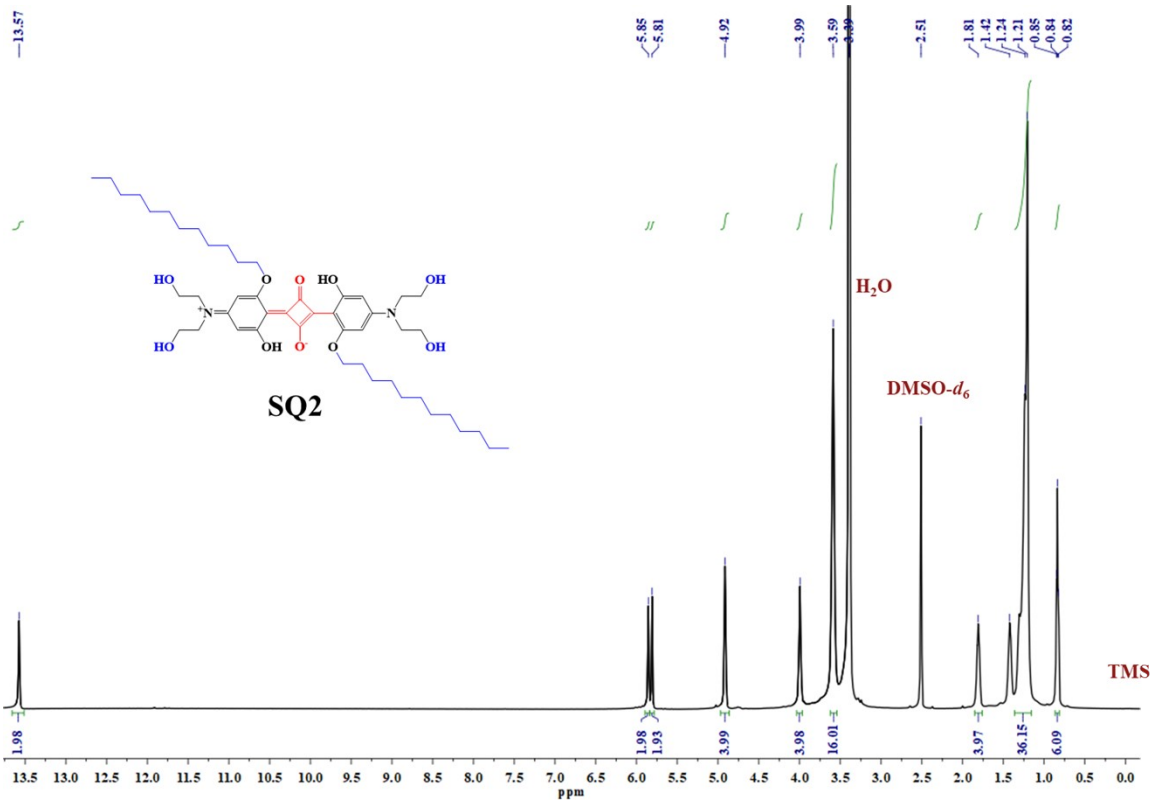

Fig. S34. ^{1}H NMR spectrum of the fluorophore SQ2 in DMSO-d_6.

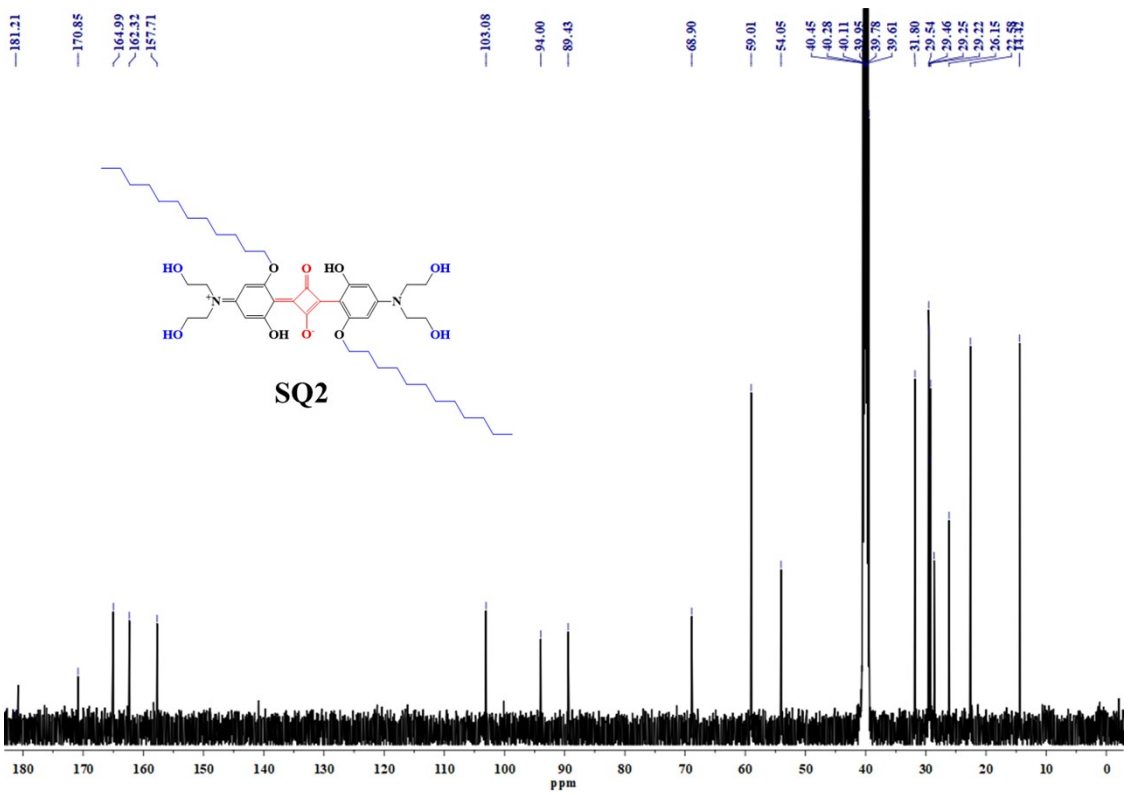

Fig. S35. ^{13}C NMR spectrum of the fluorophore SQ2 in DMSO-d_6.

11. HRMS spectra of the compounds

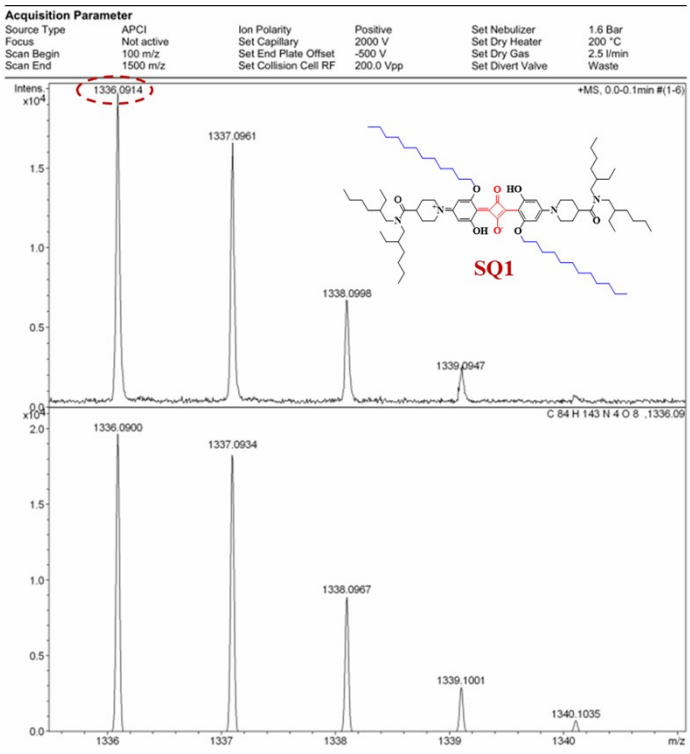

Fig. S36. HRMS spectrum of the fluorophore SQ1.

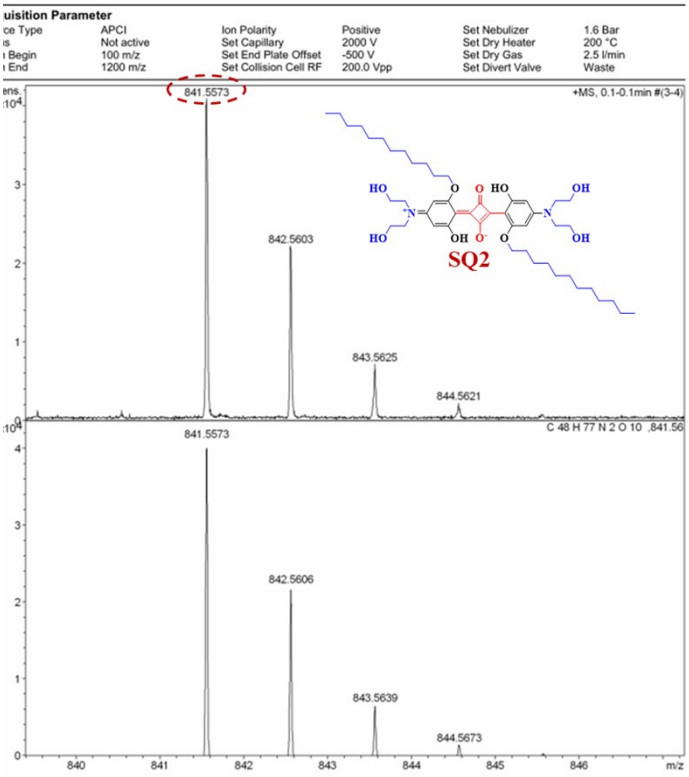

Fig. S37. HRMS spectrum of the fluorophore SQ2.

Table S2. Performance comparison of present SQs for cellular imaging with the previously reported works.

Fluorophore	$\lambda_{Abs}/\lambda_{em}$ (nm)	Wettability	Selectivity	Incubation Time	References
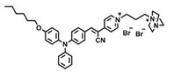	525 / 675	hydrophobicity	plasma membranes	5 min	*Chem. Sci.*, **2023**, *14*, 2139-2148
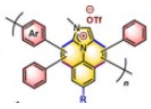	440 / 470	hydrophobicity	plasma membranes	20 min	*ACS Appl. Mater. Interfaces*, **2024**, Doi: 10.1021/acsami.3c16257
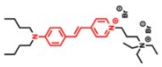	497 / 635	hydrophobicity	plasma membranes	20 min	*Bioconjugate Chem.*, **2020**, *31*, 875-883
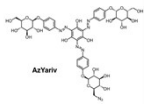	400 / 510	hydrophilicity	phloem, epidermal, and bundle sheath cells	10 min	*Bioconjugate Chem.*, **2023**, *34*, 1398-1406
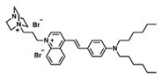	557 / 676	hydrophobicity	plasma membranes	10 min	*J. Mater. Chem. B*, **2024**, *12*, 2761-2770
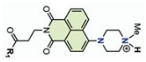	405 / 540	hydrophobicity	chloroplast	---	*Chem. Commun.*, **2022**, *58*, 1685-1688
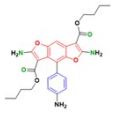	275 / 426	hydrophilicity	cell wall	20 min	*Dyes Pigm.*, **2022**, *199*, 110071
	642 / 672	hydrophobicity	cell wall (onion)	5 min	Present Work
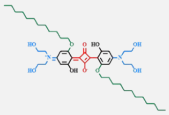	642 / 675	amphiphilicity	vacuole and nucleus (onion) cortex (seedling)	5 min	Present Work
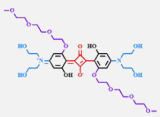	642 / 673	hydrophilicity	vacuole (onion) xylem (seedling)	5 min	Present Work

References

[1] N. Zhang, L. Liu, H. Chang, K. Liu, T. Liu, L. Ding, Y. Fang. *J. Phys. Chem. Lett.* **2023***, 14,* 7283-7289.

[2] W. Feng, L. Liu, J. Zang, W. Gang, R. Miao, L. Ding, T. Liu, J. Kong, Y. Fang. *ACS Appl. Mater. Interfaces* **2021**, *13*, 28985-28995.

[3] T. Liu, X. Liu, Y. Zhang, M. V. Bondar, Y. Fang, K. D. Belfield. *Eur. J. Org. Chem*. **2018**, 4095-4102.

[4] J. Zang, W. Feng, X. Chang, K. Liu, H. Peng, L. Ding, T. Liu, Y. Fang. *Dyes Pigm*. **2021**, *193*, 109487.

[5] T. Liu, L. Yang, J. Zhang, K. Liu, L. Ding, H. Peng, K. D. Belfield, Y. Fang. *Sens. Actuators B* **2019**, *292*, 88-93.

[6] H.-J. Chang, M. V. Bondar, T. Liu, X. Liu, S. Singh, K. D. Belfield, A. Sheely, A. E. Masunov, D. J. Hagan, E. W. Van Stryland. *ACS Omega* **2019**, *4*, 14669-14679.

[7] S. I. Klein, B. F. Molino, M. Czekaj, C. J. Gardner, V. Chu, K. Brown, R. D. Sabatino, J. S. Bostwick, C. Kasiewski, R. Bentley, *et al*. *J. Med. Chem*. **1998**, *41*, 2492-2502.

[8] P. Zlatoidsky, T. Maliar. *Eur. J. Med. Chem*. **1999**, *34*, 1023-1034.

[9] N. Wu, J. Lan, L. Yan, J. You. *Chem. Commun*. **2014**, *50*, 4438-4441.

[10] K. J. Wallace, M. Gray, Z. Zhong, V. M. Lynch, E. V. Anslyn. *Dalton Trans*. **2005**, 2436-2441.

[11] M. A. Albota, C. Xu, W. W. Webb. *Appl. Opt*. **1998**, *37*, 7352-7356.